In vitro cellular models for neurotoxicity studies:
neurons derived from P19 cells

Dina Popova

Department of Pharmacology and Clinical Neuroscience
Umeå 2017

Responsible publisher under Swedish law: the Dean of the Medical Faculty

ISBN: 978-91-7601-659-6
ISSN: 0346-6612
New Series No. 1877
Elektronisk version tillgänglig på http://umu.diva-portal.org/
Tryck/Printed by: Print & Media
Umeå, Sweden 2017

To my family

Contents

Original papers

I. **Dina Popova**, Stig O.P. Jacobsson. A fluorescence microplate screen assay for the detection of neurite outgrowth and neurotoxicity using an antibody against βIII-tubulin. Toxicology in Vitro. 2014 April; 28 (3): 411-418.

II. **Dina Popova**, Jessica Karlsson, Stig O.P. Jacobsson. Comparison of neurons derived from mouse P19, rat PC12 and human SH-SY5Y cells in the assessment of chemical- and toxin-induced neurotoxicity. Manuscript.

III. **Dina Popova,** Andréas Forsblad, Sanaz Hashemian, Stig O.P. Jacobsson. Non-serotonergic neurotoxicity by MDMA (ecstasy) in neurons derived from mouse P19 embyonal carcinoma cells. PLOS ONE. 2016 November; 11 (11): e0166750.

IV. **Dina Popova**, Stig O.P Jacobsson. *In vitro* toxicity of piperazine-derived designer drugs in differentiated neural cell lines. Manuscript.

Abstract

Humans are exposed to a variety of chemicals including environmental pollutants, cosmetics, food preservatives and drugs. Some of these substances might be harmful to the human body. Traditional toxicological and behavioural investigations performed in animal models are not suitable for the screening of a large number of compounds for potential toxic effects. There is a need for simple and robust *in vitro* cellular models that allow high-throughput toxicity testing of chemicals, as well as investigation of specific mechanisms of cytotoxicity. The overall aim of the thesis has been to evaluate neuronally differentiated mouse embryonal carcinoma P19 cells (P19 neurons) as a model for such testing. The model has been compared to other cellular models used for neurotoxicity assessment: retinoic acid-differentiated human neuroblastoma SH-SY5Y cells and nerve growth factor-treated rat pheochromocytoma PC12 cells. The chemicals assessed in the studies included the neurotoxicants methylmercury, okadaic acid and acrylamide, the drug of abuse MDMA ("ecstasy") and a group of piperazine derivatives known as "party pills". Effects of the chemicals on cell survival, neurite outgrowth and mitochondrial function have been assessed.

In Paper I, we describe a fluorescence-based microplate method to detect chemical-induced effects on neurite outgrowth in P19 neurons immunostained against the neuron-specific cytoskeletal protein βIII-tubulin. In Paper II, we show that P19 neurons are more sensitive than differentiated SH-SY5Y and PC12 cells for detection of cytotoxic effects of methylmercury, okadaic acid and acrylamide. Additionally, in P19 neurons and differentiated SH-SY5Y cells, we could demonstrate that toxicity of methylmercury was attenuated by the antioxidant glutathione. In Paper III, we show a time- and temperature-dependent toxicity produced by MDMA in P19 neurons. The mechanisms of MDMA toxicity did not involve inhibition of the serotonin re-uptake transporter or monoamine oxidase, stimulation of 5-HT_{2A} receptors, oxidative stress or loss of mitochondrial membrane potential. In Paper IV, the piperazine derivatives are evaluated for cytotoxicity in P19 neurons and differentiated SH-SY5Y cells. The most toxic compound in both

cell models was TFMPP. In P19 neurons, the mechanism of action of TFMPP included loss of mitochondrial membrane potential. In conclusion, P19 neurons are a robust cellular model that may be useful in conjunction with other models for the assessment of chemical-induced neurotoxicity.

Populärvetenskaplig sammanfattning

Det moderna samhället är beroende av kemikalier som läkemedel, bekämpningsmedel, personliga hygienprodukter samt andra industritillverkade produkter. Det finns många fördelar med dessa kemikalier såsom att läkemedel räddar liv, förbättrar livskvalitet och att bekämpningsmedel inom jordbruket gör det möjligt att massproducera mat. Nackdelarna med vissa kemikalier innefattar deras negativa påverkan på miljön och människors hälsa. En kategori av kemiska substanser som har skadliga effekter på hälsan är missbruksdroger. Antalet nya kemiska substanser som används i berusningssyfte har ökat globalt under de senaste åren och många gånger saknas det information om deras toxiska effekter. Det är viktigt att testa kemikalier i allmänhet, och missbruksdroger i synnerhet, för att förstå deras toxiska effekter och för att kunna hantera och förebygga hälso- och miljöproblem associerade med dessa kemikalier. En viktig parameter att testa är kemikaliepåverkan på nervsystemet, eftersom intag av vissa substanser kan leda till svårigheter med inlärning, minne, språk och kommunikation.

Traditionella toxikologiska undersökningar har utförts på djur. Sådana studier är dyra, tidskrävande och kan orsaka lidande hos djuren. Det finns därför behov av alternativa modeller för att utföra toxikologisk riskbedömning av kemikalier. *In vitro* cellmodeller kan användas för att testa ett flertal kemikaliers toxicitet med relativt enkla metoder och under en rimlig tid. Resultaten av dessa tester kan användas för att prioritera substanserna för vidare undersökningar i komplexa djurmodeller. Därmed kan man minska användningen av djur för toxikologiska studier.

I denna avhandling har vi utvärderat embryonala P19-karcinomceller från mus som en modell för att undersöka neurotoxiska effekter av kemikalier. Behandlingen med retinoinsyra (en nedbrytningsprodukt av vitamin A) gör att P19-celler mognar till nervliknande celler (P19-neuroner). I den första studien utvecklade vi en enkel metod för att mäta kemikaliepåverkan på neuritutväxt i P19-neuronen, eftersom skador på neuritnätverk, som är ett kommunikationsnät mellan cellerna, kan leda till

försämringar i kognitiva funktioner hos människor och djur. Vi märkte P19-neuronen med antikroppar mot det neuronspecifika cytoskelettproteinet βIII-tubulin och mätte cellernas fluorescens i en fluorescensplattläsare. Resultatet visade att metoden kunde användas för att mäta neuritutväxt och kemikaliepåverkan på neuritutväxt i P19-neuronen.

I de efterföljande studierna testade vi förmågan hos P19-neuronen att detektera toxicitet hos de kända neurotoxiska kemikalierna metylkvicksilver, okadasyra, akrylamid, missbruksdrogen MDMA (3,4-metylendioximetamfetamin) samt piperazinderivater. Vi jämförde också P19-neuronen med etablerade *in vitro* cellmodeller för att detektera toxiska effekter hos vissa av dessa substanser. Dessa cellmodeller var retinoinsyrabehandlade SH-SY5Y-celler från människa och nervtillväxtfaktorstimulerade PC12-celler från råtta. Generellt sett visade fler av de undersökta substanserna toxicitet i P19-neuronen än i de andra cellmodellerna. Vi kunde också identifiera vissa kända mekanismer bakom toxicitet för några av dessa kemikalier i P19-neuronen.

Sammanfattningsvis visar studierna att P19 neuronen är användbar som cellmodell för att undersöka neurotoxiska effekter av kemikalier och mekanismer bakom toxiciteten på cellnivå.

Abbrevations

5-HT	5-hydroxytryptamine (serotonin)
BZP	1-benzylpiperazine
Calcein-AM	calcein-acetoxymethyl
cDNA	complementary deoxyribonucleic acid
DA	dopamine
DAPI	4′,6-diamidino-2′-phenylindole dihydrochloride
DMSO	dimethyl sulfoxide
DNA	deoxyribonucleic acid
ELISA	enzyme-linked immunosorbent assay
GABA	gamma-aminobutyric acid
GSH	glutathione
LDH	lactate dehydrogenase
MAO	monoamine oxidase
MDMA	3,4-methylenedioxymethamphetamine
MeHg	methylmercury
MeOPP	1-(4-methoxyphenyl)piperazine
mRNA	messenger ribonucleic acid
MTT	3-(4,5-dimethyl-2-thiazolyl)-2,5-diphenyl-2H-tetrazolium bromide
NA	noradrenaline
NGF	nerve growth factor
PCR	polymerase chain reaction
pFPP	1-(4-fluorophenyl)piperazine
PI	propidium iodide
RNA	ribonucleic acid
SERT	serotonin transporter
TFMPP	1-(3-trifluoromethylphenyl)piperazine
TMRE	tetramethylrhodamine ethyl ester

Introduction

In vitro cellular models for toxicity assessment of chemicals

Modern society is dependent on a variety of chemicals including pharmaceuticals, pesticides, personal care products and other industrial products. There are a lot of benefits associated with these products including healthcare improvements and large-scale production of food. On the other hand, some of the chemicals are harmful to humans and animals, the environment and the ecosystems (Blaauboer, 2002). A special category of chemicals that are hazardous to humans are drugs of abuse. The production and consumption of new psychoactive substances are increasing globally (Zawilska, 2015), and the internet allows trading with those chemicals across borders (Forman *et al.*, 2006). The main customer group of these recreational substances, with poorly characterized toxic effects, are young adults. It is important to assess rapidly the toxicity of chemicals in general, and drugs of abuse in particular, and to provide that information to society. Impact of chemicals on the nervous system is an important parameter to assess the risk of cognitive abnormalities and overt brain damage that can follow the uncontrolled use of such compounds.

Traditionally, toxicological tests have been performed on animal models. The investigations on animals are expensive, time-consuming and may cause animal suffering. The toxicological data received from the animal models is to some degree uncertain when extrapolated to humans due to interspecies variabilities (Olson *et al.*, 2000; Blaauboer, 2002). There is a need for alternative approaches including *in vitro* cellular models for toxicity risk assessment not only to reduce animal testing, but also to evaluate chemicals for potential toxicity in a high-throughput manner (Judson *et al.*, 2014). Advantages of the cellular models for toxicological evaluation of chemicals include the relatively low cost of experiments that are straightforward to perform, and allow the evaluation of many chemicals within a reasonable time frame. Moreover, such models provide a tool to investigate mechanisms of toxicity

on the cellular level that are difficult to perform in more complex animal models (Harry & Tiffany-Castiglioni, 2005; Judson *et al.*, 2014).

Disadvantages of the *in vitro* cellular models for neurotoxicity assessment include their isolated context, and the lack of the processes of absorption, distribution, metabolism and excretion that occur in animals and humans. Therefore, the cellular models cannot be used to replace animal models (Blaauboer, 2002). However, *in vitro* cellular models might be an effective way of screening chemicals for potential toxicity in order to prioritize the compounds for further investigation *in vivo* (Harry & Tiffany-Castiglioni, 2005).

The development of *in vitro* systems has progressed from simple cell cultures to complex 3D structures such as human pluripotent stem cell-derived 3D neural constructs for neurotoxicity assessment (Schwartz *et al.*, 2015) and organ-on-a-chip systems (Cho & Yoon, 2017). Nevertheless, until these models become broadly available, characterized and validated for toxicological screening of chemicals, it is valuable to use simple and robust cellular models for toxicity screening of chemicals. However, even the less complex models such as human embryonic stem cells and induced pluripotent stem cells are, so far, expensive to culture and the differentiation process is long (1-3 months) (Hu *et al.*, 2010). There is thus a place for simpler, but robust, cellular model systems for *in vitro* neurotoxicity assessment of chemicals. In this respect, rat pheochromocytoma PC12 and human neuroblastoma SH-SY5Y cells have been extensively used both in undifferentiated and neuronally differentiated states (Slotkin *et al.*, 2007; Parran *et al.*, 2003; Gustafsson *et al.*, 2010; Barbosa *et al.*, 2014). The present thesis advances the argument that retinoic acid-treated mouse embryonal carcinoma P19 cells are also a useful model for neurotoxicity assessment. The detailed information about these cell types as well as chemicals used for evaluation of the model are presented below.

P19 cells and retinoic acid-treated P19 cells

P19 cells are embryonal carcinoma cells from the C3H/He mouse strain. They originated from the tumour obtained after the transplantation of a 7.5 day embryo into the testis of a male mouse. The teratocarcinoma was removed, dissected and cultured. P19 cells were derived from undifferentiated stem cells established in the cell culture (McBurney & Rogers, 1982).

P19 cells can *in vitro* differentiate to cells from all three germ layers: endoderm, mesoderm and ectoderm, depending on the treatment (McBurney *et al.*, 1982; Smith *et al.*, 1987; Jones-Villenueve *et al.*, 1982). Dimethyl sulfoxide (DMSO) induces their differentiation into cardiac and skeletal muscle cells (McBurney *et al.*, 1982). Retinoic acid induces differentiation of P19 cells to neurons, astrocytes and fibroblast-like cells (Jones-Villeneuve *et al.*, 1982). When serum-free medium is used, the neuronal cells cultures are mostly free of glial or fibroblast-like cells (Yao *et al.*, 1995). P19 neurons possess a number of features characteristic of cultured mammalian brain cells. Their morphology is similar to the mammalian brain cells in culture. They have small cell bodies with long processes that resemble axons and dendrites. P19 neurons are postmitotic (McBurney *et al.*, 1988) and possess functional synapses (Finley *et al.*, 1996; Morassutti *et al.*, 1994).

Retinoic acid-treated P19 cells (P19 neurons) have several neurotransmitter phenotypes in the same population (Staines *et al.*, 1994), instead of a single or distinct co-expressed neurotransmitter(s) characteristic of neurons in the nervous system. The inhibitory neurotransmitter GABA and the enzymes glutamic acid decarboxylase and GABA-transaminase, required for GABA synthesis and degradation, respectively, have been detected (Staines *et al.*, 1994). The neuromodulator acetylcholine and the enzymes responsible for its synthesis and degradation, choline acetyltransferase and acetylcholinesterase, respectively, have also been identified in the cells (Parnas & Linial, 1995). The culture conditions define whether or not the retinoic acid-treated P19 cells differentiate into a cholinergic neuronal phenotype. When cultured at a low density of 5 x 10^4 cells/cm^2,

the cells express the enzymes choline acetyltransferase and acetylcholinesterase. Although, at a high density culture (2 x 10^5 cells/cm^2), the cholinergic phenotype is suppressed (Parnas & Linial, 1995). P19 neurons express functional ionotropic glutamate receptors of *N*-methyl-D-aspartate (NMDA) and α-amino-3-hydroxy-5-methyl-4-isoxazolepropionic acid (AMPA)/kainate type, that are characteristic of neurons in the central nervous system (Turetsky *et al.*, 1993). Functional CB1 cannabinoid receptors have been found in P19 neurons (Svensson *et al.*, 2006). Finally, the P19S18O1A1 clone of P19 cells has an adrenergic phenotype since the cells possess the enzymes in the pathway of catecholamine synthesis: tyrosine hydroxylase, dopamine-β-hydroxylase and phenylethanolamine *N*-methyltransferase (Sharma & Notter, 1988).

SH-SY5Y cells and retinoic acid-differentiated SH-SY5Y cells

SH-SY5Y is a human neuroblastoma cell line, a subclone of SK-N-SH cells established in 1970 from a bone marrow aspiration of a 4-year-old girl diagnosed with metastatic neuroblastoma (Biedler *et al.*, 1973). SH-SY5Y cells are catecholaminergic neuroblastoma that possess moderate levels of dopamine-β-hydroxylase activity, express tyrosine hydroxylase and the dopamine transporter protein (Biedler *et al.*, 1978; McMillan *et al.*, 2007; Takahashi *et al.*, 1994). SH-SY5Y cells can also covert glutamate to GABA (Biedler *et al.*, 1978). Upon exposure to retinoic acid, SH-SY5Y cells differentiate to a mature dopaminergic-like neurotransmitter phenotype. Both undifferentiated and retinoic acid-differentiated SH-SY5Y cells produce dopamine, but the dopamine levels are increased in the differentiated cells. The retinoic acid-differentiated SH-SY5Y cells possess dopamine and noradrenaline neurotransmitter transporters (Korecka *et al.*, 2013) as well as functional muscarinic receptors (Fowler *et al.*, 1989).

Undifferentiated and differentiated SH-SY5Y cells have been used for neurotoxicity assessment of chemicals (Gustafsson *et al.*, 2010; Barbosa *et al.*, 2014). Both cell types have also been applied for Parkinson's disease studies due to their dopaminergic properties (Lopes *et al.*, 2010). Moreover, the cells have been used in

Alzheimer's disease studies since tau isoforms and amyloid beta proteins are present in both undifferentiated and differentiated SH-SY5Y cells (Agholme *et al.*, 2010).

PC12 cells and nerve growth factor-treated PC12 cells

PC12 is a single cell clonal line established from a pheochromocytoma of the rat adrenal medulla (Greene & Tischler, 1976). Upon exposure to the nerve growth factor (NGF) protein, PC12 cells stop proliferating and form neuron-like processes. The effects of NGF are reversible. Its removal from the culture medium leads to neurite degeneration, but leaves cell bodies unaffected, and the cells begin to divide some days after NGF removal (Greene & Tischler, 1976).

PC12 cells and NGF-stimulated PC12 cells express the enzymes for catecholamine synthesis: tyrosine hydroxylase, DOPA decarboxylase and dopamine-β-hydroxylase. As a result, PC12 cells and NGF-treated PC12 cells synthesize dopamine but also noradrenaline and therefore resemble sympathetic neurons (Greene & Tischler, 1976; Fujita *et al.*, 1989).

PC12 cells synthesize, store and release acetylcholine (Greene & Rein, 1977), and possess the functional enzymes responsible for its synthesis and degradation, choline acetyltransferase and acetylcholinesterase, respectively. NGF increases the activity of both enzymes in PC12 cells (Schubert *et al.*, 1977; Rieger *et al.*, 1980), and the cells are able to form cholinergic synapses with the clonal cell line L6 of skeletal muscle origin (Schubert *et al.*, 1977).

PC12 cells are a useful model to study regulation of neurite development and the process of neuronal differentiation (Greene & Tischler, 1976; Fujita *et al.*, 1989). The cell model has also been used to study developmental neurotoxicity of chemicals (Slotkin *et al.*, 2007; Parran *et al.*, 2003).

Methylmercury

Mercury (Hg) is listed among top 10 hazardous chemicals for public health by the World Health Organization (World Health Organization, 2016). The organic form of mercury that is particularly toxic to humans is methylmercury (MeHg). Inorganic mercury is transformed into organic MeHg in bacteria (Schaefer *et al.*, 2011; Parks *et al.*, 2013), and accumulates in fish and other marine organisms (Clayden *et al.*, 2015; Souza-Araujo *et al.*, 2016). Humans are exposed to MeHg primarily via dietary consumption of seafood.

Human exposure

Sheehan *et al.*, 2014 identified three categories of seafood-consuming populations of women and infants with greatest health concerns from MeHg exposure. Those categories were (1) rural populations living at the riverside next to tropical small-scale gold mining operations whose diets are based on local freshwater fish*;* (2) people in Arctic regions that consume marine mammals on a regular basis*;* and (3) populations at the coasts of the Pacific Ocean and the Mediterranean Sea, who consume commercially available seafood.

Acute exposure to MeHg (high concentrations)

The first documented case of epidemic MeHg poisoning occurred in Japan around Minamata Bay in the early 1950s. MeHg was released into Minamata Bay from a chemical factory, and the population was exposed to high concentrations of MeHg via consumption of polluted fish. The levels of mercury in local marine products were high (6-36 µg/g) (Harada, 1995) compared to less than 0.5 µg/g found in most fish nowadays (FDA, 2017).

In some cases, the poisoning resulted in a severe neurological disease named Minamata disease. The symptoms included cerebellar ataxia (uncoordinated movements and difficulties in writing and speaking), blurred vision, impaired

hearing, numbness in hands and feet and intellectual/personality disabilities. Intellectual and emotional disabilities were severe in some of the cases. Children born to mothers exposed to MeHg showed marked disturbances in mental and motor development (Harada, 1995). Thereby, MeHg was considered highly toxic to the human brain and especially toxic to the nervous system in the developing fetus (Ekino *et al.*, 2007).

Further evidence for MeHg neurotoxicity came after acute MeHg poisoning in rural Iraq in 1972. The population was exposed via bread made from wheat treated with fungicide that contained MeHg. The levels of mercury in blood were higher in infants exposed *in utero* compared to their mothers. In severe cases, the infants had largely impaired motor and mental functions (Amin-Zaki *et al.*, 1974).

Chronic exposure to MeHg (moderate and low concentrations)

In both cases (Japan and Iraq) described above, the populations were acutely exposed to high concentrations of MeHg. The question was raised if prenatal exposure to lower concentrations of MeHg had an effect on children's neuronal development. Two large cohort studies were performed in order to answer that question. These were the studies in the Faroe Islands and in the Seychelles. In the Faroe Islands, exposure to MeHg primarily comes from the consumption of whale meat, and in the Seychelles, the diet is essentially based on fish.

The results of these investigations differed. The Faroe Island study showed that prenatal exposure to MeHg had adverse effects on the cognitive functions in children such as language, attention and memory (Grandjean *et al.*, 1997). However, in the Seychelles, no association was found between MeHg exposure and adverse effects on neuronal development (van Wijngaarden *et al.*, 2013; Strain *et al.*, 2015). The difference might be partly due to higher MeHg concentrations in whale (Julshamn *et al.*, 1987) than in fish (FDA, 2017) as well as other environmental contaminants in whale that could possibly affect neuronal development.

While adverse effects of prenatal exposure to MeHg in humans have been debated based on the results of these two important studies, investigations made on animals and cellular models continue to gather evidence for neurotoxic effects of MeHg.

Studies in animals and in cellular models

MeHg is particularly toxic to the developing brain. The chemical affects nerve cells in several brain regions. In rat brain, during neuronal development, MeHg inhibited neurite outgrowth in the cerebellum (Fujimura *et al.*, 2016), disrupted neuronal migration in cerebrocortical neurons (Guo *et al.*, 2013), and induced apoptosis in the hippocampus (Sokolowski *et al.*, 2011).

In *in vitro* cellular models, MeHg showed similar cytotoxicity as observed *in vivo* i.e. disrupted neurite formation and cell death. Thus, in rat primary embryonic cortical neural stem cells, MeHg inhibited neuronal differentiation at a low nanomolar concentration (5 nM) and induced apoptosis at a low micromolar concentration (0.5 μM) (Tamm *et al.*, 2006). In rat neural progenitor cells of embryonic cerebral cortex, MeHg (10 nM) suppressed cell proliferation (Fujimura & Usuki, 2015). In the mouse hippocampal HT22 cell line, MeHg (4 μM) caused necrotic and apoptotic cell death (Tofighi *et al.*, 2011).

Molecular mechanisms of MeHg neurotoxicity are complex and closely interconnected. They key events are presented in Table 1.

A number of mechanistic studies cited in the Table have been performed on cellular models that are particularly useful for investigation of specific mechanisms of toxicity.

Table 1. Molecular mechanisms of MeHg neurotoxicity.

Molecular mechanism	Reference
Glutamate excitotoxicity	
Increased extracellular glutamate levels	
Enhanced sensitivity of NMDA receptors	Carratu *et al.*, 2006
Inhibited glutamate uptake	Manfroi *et al.*, 2004
Modulations of intracellular Ca^{2+} levels	
Increased $[Ca^{2+}]_i$ levels	Limke & Atchison, 2002
Mitochondrial dysfunctions	
Decreased mitochondrial Ca^{2+} uptake	
Decreased ATP levels	
Loss of mitochondrial membrane potential ($\Delta\Psi m$)	Tofighi *et al.*, 2011
Oxidative stress	Caballero *et al.*, 2016
Disruption in development of glutathione antioxidant system	
Decreased GSH levels	
Inhibited glutathione peroxidase activity	
Inhibited glutathione reductase activity	Stringari *et al.*, 2008
Apoptosis	
Bax activation	
Cytochrome c release	Tamm *et al.*, 2006
Caspase activation	Sokolowski *et al.*, 2011

Abbreviations: $[Ca^{2+}]_i$, intracellular Ca^{2+}; ATP, adenosine triphosphate; GSH, glutathione.

Okadaic acid

Okadaic acid is a marine biotoxin found in microalgae dinoflagellates. It accumulates in shellfish and is responsible for diarrhetic shellfish poisoning (Nielsen *et al.*, 2016). Okadaic acid is a potent and selective reversible inhibitor of two major serine/threonine protein phosphatases PP1 and PP2A with a higher affinity for PP2A (Bialojan & Takai, 1988; Sasaki *et al.*, 1994). The inhibition of these phosphatases leads to hyperphosphorylation of a large number of proteins, thereby changing their function (Haystead *et al.*, 1989). For example, okadaic acid leads to activation of major kinases in neurons associated with hyperphosphorylation of the tau protein, a property that has been exploited in experimental Alzheimer's disease research (Kamat *et al.*, 2014).

The neurotoxic effects of okadaic acid are summarized in Table 2.

Table 2. Neurotoxic effects of okadaic acid *in vivo* and *in vitro.*

	Reference	
Neurotoxic effect	***In vivo***	***In vitro***
Cytoskeletal disruption	Arias *et al.*, 1998	Merrick *et al.*, 1997
Oxidative stress	Zhang & Simpkins, 2010	Yi *et al.*, 2009
Mitochondrial dysfunction	Kamat *et al.*, 2011	Yoon *et al.*, 2006
Apoptosis	Kamat *et al.*, 2011	Cagnoli *et al.*, 1996

The cytoskeleton is one of the key targets of okadaic acid. In cortical neurons derived from rat pups and NGF-stimulated PC12 cells, okadaic acid inhibited neurite outgrowth at low nanomolar concentrations (Das & Miller, 2012; Chiou & Westhead, 1992). In cultured rat cortical neurons and in a human neuroblastoma cell line (MSN), okadaic acid induced changes in neuronal cytoskeleton that resulted in cell death (Arias *et al.*, 1993). In the human neuroprogenitor cell line NT2N,

okadaic acid depolymerized stable microtubules and produced degeneration of axons (Merrick *et al.*, 1997). *In vivo* in the rat hippocampus, okadaic acid caused loss of the microtubule-associated protein MAP2, neurodegeneration and cell death (Arias *et al.*, 1998).

Acrylamide

Acrylamide is a synthetic monomer used for production of polyacrylamide that has applications in a number of industries including paper manufacturing, wastewater treatment and mining. Acrylamide is also formed when the carbohydrate-rich food is prepared at temperatures above 120 °C such is the case with frying, grilling and baking (Taeymans *et al.*, 2004; Sharp, 2003).

Acrylamide is neurotoxic to humans (He *et al.*, 1989; Bachmann *et al.*, 1992) and experimental animals (Jangir *et al.*, 2016; Tian *et al.*, 2015; Ko *et al.*, 1999). In humans, factory workers exposed to acrylamide showed neurotoxic symptoms including numbness of the hands and feet, muscle weakness, unsteady walking and clumsiness in the hands (He *et al.*, 1989; Bachmann *et al.*, 1992). In animal studies, acrylamide induced weakness of the hind limbs, uncoordinated movements, loss of pain sensation, increase in latency to move and increased freezing time (Jangir *et al.*, 2016; Ko *et al.*, 1999). In the rat brain, exposure to acrylamide (15 mg/kg/day for 28 days via oral gavage) caused neuronal degeneration, separation of nerve fibers, aggregation of glial cells and necrosis. In the spinal cord, demyelination of gray matter and liquefaction of white matter were observed (Jangir *et al.*, 2016). The *in vitro* and *in vivo* neurotoxic effects of acrylamide are summarized in Table 3.

Table 3. Neurotoxic effects of acrylamide *in vivo* and *in vitro*.

	Reference	
Neurotoxic effect	***In vivo***	***In vitro***
Oxidative stress	Lakshmi *et al.*, 2012	Pan *et al.*, 2015
Apoptosis	Lakshmi *et al.*, 2012	Komoike & Matsuoka, 2016

Acrylamide is an α,β-unsaturated carbonyl derivative that belongs to the chemical class of type-2 alkenes. It is an electrophile that forms covalent bonds with nucleophilic residues on biologic macromolecules including enzymes (LoPachin & Gavin, 2012). It preferentially interacts with sulfhydryl side-chains on cysteine residues (Barber & LoPachin *et al.*, 2004; Barber *et al.*, 2007). The sulfhydryl groups located in the catalytic centres (in particular catalytic triads) of enzymes often react faster with the electrophiles, compared to the majority of sulfhydryl groups in proteins that are primarily present in other regions. Many of these catalytic triads are found in critical enzymes in nerve terminals (LoPachin & Barber, 2006). Acrylamide binding to the sulfhydryl groups in the catalytic triads will result in abnormal enzyme function and hence neurotransmission, the net outcome being to produce neurotoxicity (Barber & LoPachin, 2004; Barber *et al.*, 2007; LoPachin *et al.*, 2004).

Acrylamide is also toxic during neuronal development. Rat pups born to mothers exposed to 15 mg/kg/day of acrylamide by oral gavage from gestational day 6 to lactational day 10, showed decreased horizontal activity and auditory startle response (Wise *et al.*, 1995). *In vitro*, acrylamide reduced neurite outgrowth in retinoic acid-differentiated human neuroblastoma SH-SY5Y cells and differentiated mouse neural progenitor cells C17. 2 (Attoff *et al.*, 2016).

MDMA ("ecstasy")

3,4-Methylenedioxymethamphetamine (MDMA), also called "ecstasy" is a popular recreational drug that has been used since the 1980s (Pentney, 2001). The compound is neurotoxic to both humans and animals. The most pronounced acute toxic effect produced by MDMA is hyperthermia (elevated body temperature) (Hall & Henry, 2006; Fantegrossi *et al.*, 2003; Green *et al.*, 2005). Ambient temperature also affects MDMA neurotoxiciy in laboratory animals (Malberg & Seiden, 1998) and in rat cortical neurons (Capela *et al.*, 2006).

In the European Union the prevalence rates of ecstasy use in the 15-34-year-old age group based on national surveys since 2012 ranged from 0.1 % in Italy to 3 % in the United Kingdom (Mounteney *et al.*, 2016).

In the United States, 0.8 % (270 000) of young adults aged 18 to 25 years were current users of ecstasy in 2014 according to the results from the National Survey on Drug Abuse and Health (Center for Behavioral Health Statistics and Quality, 2015).

The visits to the emergency department related to ecstasy in selected metropolitan areas in the USA doubled between 2004 and 2011, from around 10,000 to 22,500 visits, respectively, reflecting the trend in drug abuse (Substance Abuse and Mental Health Services Administration, 2013).

The acute toxic effects of ecstasy vary from common minor side effects to rare but potentially life-threatening conditions. The majority of users have minor side effects as tachycardia, dry mouth and bruxism (Peroutka *et al.*, 1988). The severe effects include sudden death, hyperpyrexia leading to rhabdomyolysis and multiple organ failure (Henry *et al.*, 1992), the serotonin syndrome (Parrott, 2002), acute liver failure (Milroy *et al.*, 1996), panic disorder (Pallanti & Mazzi, 1992), hyponatremia and cerebral edema (Hartung *et al.*, 2002).

The long-term neurotoxic effects of MDMA vary between the species. In non-human primates (Ricaurte *et al.*, 1988) and rats (Battaglia *et al.*, 1987; O'Hearn *et al.*, 1988), serotonergic neurons are predominantly damaged. In rat brain, MDMA produces long-term structural and functional damages to serotonergic nerve terminals (Battaglia *et al.*, 1987; O'Hearn *et al.*, 1988). However, in mice, dopaminergic and serotonergic neurons are affected, depending on the mouse strain and the investigated brain region (Granado *et al.*, 2008; O'Callaghan & Miller, 1994; Zhang *et al.*, 2006).

The research about MDMA neurotoxicity has mostly been focused on the monoamine system, especially on serotonergic neurons in the brain. Both *in vivo*

(Gudelsky & Nash, 1996; Hagino *et al.*, 2011) and *in vitro* (Fitzgerald & Reid 1990, Johnson *et al.*, 1991, Steele *et al.*, 1987), MDMA increases extracellular levels of serotonin and dopamine by acting on the serotonin and dopamine transporter proteins, respectively. *In vitro*, MDMA also releases noradrenaline via the noradrenaline transporter (Table 4). Additionally, MDMA inhibits the enzyme monoamine oxidase (Leonardi & Azmitia, 1994) that metabolizes serotonin, dopamine and noradrenaline (Nagatsu, 2004). This contributes to elevated levels of these neurotransmitters in the brain and disturbs the brain neurochemistry. 5-HT_{2A} receptors are also involved in MDMA neurotoxicity. Ketanserine, the 5-HT_{2A} receptor antagonist, reduced MDMA toxicity in the rat brain *in vivo* (Shioda *et al.*, 2008) and in rat cortical neuronal cultures *in vitro* (Capela *et al.*, 2006).

The mechanisms of MDMA neurotoxicity are complex and not completely clarified. Besides hyperthermia and dysfunctions in the monoamine system, the formation of toxic metabolites (Capela *et al.*, 2007), glutamate excitotoxicity (Anneken & Gudelsky, 2012; Anneken *et al.*, 2013), inflammation (Orio *et al.*, 2004), mitochondrial dysfunction (Puerta *et al.*, 2010; Alves *et al.*, 2009) and oxidative stress (Colado *et al.*, 1997; Shankaran *et al.*, 1999) contribute to MDMA neurotoxicity.

Benzylpiperazine-based "party pills"

Benzylpiperazine (BZP) is a stimulant drug of abuse with amphetamine-like subjective effects (Bye *et al.*, 1973). The compound became popular in New Zealand (Wilkins *et al.*, 2006) in the early 2000s where it had a legal status until the year 2008. BZP was the main ingredient of so called "party pills", that were easily available in New Zealand in a wide range of outlets such as grocery stores and liquor shops. "Party pills" gained popularity among young adults and were considered to be "safe", largely because of their legal status (Wilkins *et al.*, 2006; Sheridan & Butler, 2010). In Europe, benzylpiperazine-based pills have been sold on the Internet since the year 2000 (de Boer *et al.*, 2001).

In the "party pills", BZP was often mixed with 1-(3-trifluoromethylphenyl)-piperazine (TFMPP) (Thompson *et al.*, 2006; EMCDDA, 2009). Other piperazine derivatives including 1-(3-chlorophenylpiperazine) (mCPP), 1-(3,4-methylenedioxy-benzyl)piperazine (MDBP), 1-(4-fluorophenyl)piperazine (pFPP) and 1-(4-methoxy-phenyl)piperazine (MeOPP) have also been used recreationally (EMCDDA, 2009; Zuba & Byrska, 2013).

BZP and TFMPP act on the monoamine system in the brain. BZP predominantly stimulates release of dopamine, and TFMPP evokes release of serotonin by acting on the respective protein transporters (Table 4). In rats, the combination of BZP and TFMPP mimics the mechanism of action of the recreational drug MDMA (or "ecstasy) in the brain. However, the piperazine derivatives are less potent than MDMA to evoke release of the neurotransmitters (Baumann *et al.*, 2005).

BZP-based "party pills" produce toxic effects in humans including confusion, palpitation, agitation, anxiety, insomnia and seizures (Gee *et al.*, 2005; Gee *et al.*, 2008; Thompson *et al.*, 2006). BZP increases the frequency of seizures with increased plasma concentrations. However, some individuals with low plasma concentrations develop seizures (Gee *et al.*, 2008). Severe cases of BZP intoxication that resulted in multi-organ failure have also been reported (Gee at al., 2010). However, in many cases, other drugs of abuse in addition to BZP-based "party pills" have been consumed. The polydrug abuse makes it hard to distinguish specific toxicity of BZP in humans.

In rhesus monkeys trained to self-administrate amphetamine and cocaine, symptoms of BZP intoxication include bizzare body postures, involuntary head movements and jaw chattering (Fantegrossi *et al.*, 2005). In rats, the combination of BZP and TFMPP have induced short-lived seizures upon an intravenous injection of the dose of 3 mg/kg each, followed by the dose of 10 mg/kg each 60 min later (Baumann *et al.*, 2005).

On the cellular level, in differentiated human neuroblastoma SH-SY5Y cells, the piperazine derivatives including BZP and TFMPP induced apoptotic cells death. The mechanisms of toxicity of the compounds involved increased intracellular Ca^{2+} levels, mitochondrial hyperpolarization and depletion of intracellular GSH levels. These results suggested a potential neurotoxicity of the piperazine derivatives (Arbo *et al.*, 2016).

The toxic effects of the piperazine derivatives *in vitro* are not limited to the neuroblastoma cells, but are also found in other cell types. In primary rat hepatocytes, the piperazine derivatives induced oxidative stress, GSH depletion, loss of mitochondrial membrane potential, ATP depletion and activation of caspase-3 (Dias da Silva *et al.*, 2015). In the rat cardiac cell line H9c2, the piperazine derivatives including BZP and TFMPP produced a decrease in ATP levels and an increase in intracellular Ca^{2+} levels. Additionally, TFMPP but not BZP decreased mitochondrial membrane potential in the cell line (Arbo *et al.*, 2014).

Table 4. Release of monoamine neurotransmitters by BZP, TFMPP and MDMA in the rat brain.

Compound	*In vivo*	*In vitro*	Reference
1-benzylpiperazine (BZP)	DA 5-HT	DA NA	Baumann *et al.*, 2005 Nagai *et al.*, 2007
1-(3-trifluoromethylphenyl)-piperazine (TFMPP)	5-HT	5-HT	Baumann *et al.*, 2005
3,4-methylenedioxymeth-amphetamine (MDMA)	5-HT DA	5-HT DA NA	Gudelsky & Nash, 1996 Fitzgerald & Reid, 1990

Abbreviations: DA, dopamine; 5-HT, serotonin; NA, noradrenaline.

Aims of the thesis

From the introduction, it is clear that there is a need for novel *in vitro* cellular models for neurotoxicological risk assessment of chemicals. Embryonal carcinoma P19 cells that, upon exposure to retinoic acid, differentiate to neuron-like cells (P19 neurons) are a possible candidate for such an *in vitro* model. In this thesis, P19 neurons have been evaluated for neurotoxicity testing using chemicals with known neurotoxic effects, i.e. methylmercury, okadaic acid, acrylamide, the drugs of abuse MDMA ("ecstasy") and the piperazine derivatives. Chemical-induced effects on cell viability, neurite outgrowth and mitochondrial function have been investigated. P19 neurons have also been compared to differentiated human SH-SY5Y and rat PC12 cells for their responses to the tested compounds. Effects of chemicals on neurite outgrowth is an important morphological parameter used in neurotoxicity assessment. So far, the high-throughput evaluation of neurite outgrowth requires expensive equipment and software. We have investigated if the relatively inexpensive fluorescence microplate reader can be used to rapidely measure neurite outgrowth in P19 neurons. Consequently, the aims of the study were:

Paper I. To develop a fluorescence-based microplate reader assay for a rapid detection of chemical-induced effects on neurite outgrowth in P19 neurons using anti-βIII-tubulin antibodies.

Paper II. To compare P19 neurons to differentiated human SH-SY5Y and rat PC12 cells for neurotoxicity assessment of methylmercury, okadaic acid and acrylamide.

Paper III. To investigate mechanisms of toxicity of MDMA in P19 neurons with focus on the proteins SERT and MAO, oxidative stress and mitochondrial function.

Paper IV. To examine *in vitro* toxicity of piperazine-derived designer drugs in P19 neurons and differentiated SH-SY5Y cells.

Methodological considerations

Cell lines (Paper I, II, III, IV)

P19 mouse embryonal carcinoma cells (cat. no. ECACC 95102107), PC12 rat adrenal pheochromocytoma cells (cat. no. ECACC 88022401), SH-SY5Y human neuroblastoma cells (cat. no. ECACC 94030304), Caco-2 human colon adenocarcinoma cells (cat. no. ECACC 86010202) and HepG2 human liver carcinoma cells (cat. no. ECACC 85011430) were purchased from European Collection of Authenticated Cell Cultures (ECACC). The cells were maintained in T75 cm^2 tissue culture flasks at 37 °C, 5 % CO_2.

Cell culture and differentiation of P19, SH-SY5Y and PC12 cells

P19 cells (Paper I, II, III, IV)

P19 cells were cultured in MEM-α medium with deoxyribonucleosides and ribonucleosides (αMEM) that contained 10 % fetal bovine serum (FBS), 1 % non-essential amino acids (NEAA), 100 units/ml penicillin and 100 µg/ml streptomycin (1 % PEST).

P19 cells were induced to neuronal differentiation with retinoic acid, essentially as described by Yao *et al.*, 1995, and cultured in Neurobasal medium with B27 supplement (Svensson *et al.*, 2006). Briefly, P19 cells were seeded at a density of 1×10^6 cells on bacterial-grade Petri dishes (Ø 92 mm; Sarstedt Inc., Newton, NC, USA) in αMEM containing 5 % FBS, 1 % NEAA and 1 % PEST. Differentiation was induced by incubation with 1 µM all-trans retinoic acid (RA) for 4 days. The medium was changed 2 days after the induction. The cell aggregates formed during the induction were incubated for 10 min with trypsin, dissociated and plated on 96-, 12- or 6-well plates pre-coated with poly-D-lysine (50 µg/ml). The cells were cultured at a density of 500-1000 cells/mm^2 in a serum-free Neurobasal medium

supplemented with B27 (Thermo Fisher Scientific, Invitrogen Life Technologies, Uppsala, Sweden) for 6-10 days. Half of the medium in each well was changed every 48 h.

SH-SY5Y cells (Paper II, IV)

SH-SY5Y cells were cultured in minimal essential medium with Earl´s salts (EMEM) supplemented with 10 % FBS, 1 % NEAA, 2 mM L-glutamine and 1 % PEST. Differentiation of SH-SY5Y cells was performed essentially according to the protocol of Gustafsson *et al.*, 2010. The cells were plated at a density of 500 cells/mm^2 in 96-well plates overnight in the culture medium. The medium was replaced with the differentiation medium (Dulbecco's modified medium with Ham´s F12 medium [1:1], 1 % N2 supplement and 1 % PEST) containing 1 µM RA. The cells were differentiated for 3 to 6 days. Half of the medium per well was changed every 48 h.

PC12 cells (Paper II)

PC12 cells were cultured in Dulbecco´s modified Eagle's medium with high glucose (DMEM), 10 % horse serum (HS), 1 % FBS and 1 % PEST in T75 flasks coated with poly-D-lysine (50 µg/ml). The cells, when passaged, were incubated for 5 min at 37 °C, 5 % CO_2 with 0.5 mM ethylenediaminetetraacetic acid (EDTA) solution in PBS, and then detached by gentle cell scraping. We did not trypsinize the cells since trypsin might reduce the amount of NGF receptors that are required for differentiation (Cattaneo *et al.*, 1983). For differentiation, PC12 cells were plated at a density of 500 cells/mm^2 in 96-well plates and cultured overnight. The medium was replaced with the differentiation medium (DMEM, 1 % HS and 1 % PEST) containing 100 ng/ml rat nerve growth factor β (NGFβ). Half of the medium was changed every 48 h.

Comments

In our hands, P19 cells were a robust model to study events during neuronal differentiation. The vast majority of retinoic acid-treated P19 cells possessed neuron-like morphology, were postmitotic and built a complex neural network.

SH-SY5Y cells changed the morphology and produced long neurites during differentiation with 1 μM retinoic acid, but continued to proliferate. There are several protocols in the literature for differentiation of SH-SY5Y cells. The most common chemical used for that purpose is retinoic acid (Agholme *et al.*, 2010; Korecka *et al.*, 2013). Other chemicals have also been applied for differentiation including brain-derived neurotrophic factor, nerve growth factor and vitamin D_3. Some protocols include a multiple-step procedure (Agholme *et al.*, 2010). We differentiated SH-SY5Y cells with retinoic acid, and used a simple protocol that is practical for screening of a large number of chemicals for potential neurotoxic effects.

PC12 cells generated neurites upon treatment with 100 ng/ml NGF, but a much lower proportion of cells possessed neurites compared to P19 and SH-SY5Y cells. That phenomenon has been observed in other studies as well, where mixed population of differentiated and proliferated PC12 cells, upon treatment with NGF, have been reported (Chiou & Westhead, 1992; Weber *et al.*, 2013). Although other authors have reported that the majority of NGF-treated PC12 cells generate neurites (Das *et al.*, 2004; Baskey *et al.*, 2002). Due to the discrepancies in the differentiation outcome of PC12 cells stimulated with NGF, the model should be used with caution for a standard neurotoxicity screening of chemicals.

Immunofluorescence detection of βIII-tubulin (Paper I, II, IV)

The cells were plated in black 96-well plates with clear bottoms and immunostained against βIII-tubulin, a neuron-specific protein in microtubules of the cytoskeleton (Katsetos *et al.*, 2003).

Briefly, the cells were fixed for 30 min with 4 % formaldehyde and permeabilized for 5 min with 0.1 % Triton X-100. The cells were washed three times with PBS, and non-specific binding was blocked by 30 min incubation with PBS containing 3 % fetal bovine serum. The samples were incubated for 1 h with the rabbit polyclonal antibodies against βIII-tubulin (Convance Inc., Princeton, New Jersey, USA) diluted 1:500 and washed three times with PBS. The samples were incubated for 1 h with the secondary goat anti-rabbit antibodies Alexa Fluor 488® (Invitrogen™, Uppsala, Sweden) diluted 1:250, and washed three times with PBS. Fluorescence was measured in a BMG FLOUstar Galaxy microplate reader (BMG Lab technologies, Offenburg, Germany) with 485/520 nm excitation/emission filters. The fluorescence microscopy images were obtained using a Nikon Eclipse TE2000-U inverted microscope with a Plan Fluor ELWD 20x/0.45 objective with a Nikon Digital Sight DS-5Mc camera (Tekno Optik AB, Skärholmen, Sweden). Samples exposed for 30 min to 2 % Triton X-100 at 37 °C, 5 % CO_2 were controls for the amount of fluorescence in dead cells.

Comments

The protein βIII-tubulin is present both in neurites and cell bodies. In P19 cells, that are postmitotic during the process of neuronal differentiation, the increase in βIII-tubulin fluorescence is correlated to neurite outgrowth as shown in paper I. However, in SH-SY5Y cells, that continue to proliferate during the differentiation with retinoic acid, the increase in βIII-tubulin fluorescence is due to the increased number of cells in addition to growing neurites. In differentiating PC12 cells, the lower increase in fluorescence of βIII-tubulin compared to P19 and SH-SY5Y cells, is due to less number of cells that have generated neurites (see paper II).

DAPI staining (Paper I)

The cells immunolabelled against βIII-tubulin were co-stained with 4′,6-diamidino-2-phenylindole dihydrochloride (DAPI) nuclear stain for manual counting of the number of cells. DAPI was applied at a concentration of 0.3 mM/well for 3 min.

Neurite tracing with NeuronJ plug-in for ImageJ software (Paper I)

Images of the cells immunostained against βIII-tubulin (three images per well) were obtained with a Nikon Eclipse TE2000-U inverted microscope with a Plan Fluor ELWD 20x/0.45 objective with a Nikon Digital Sight DS-5Mc camera (Tekno Optik AB, Skärholmen, Sweden). The images were converted to 800 x 600 pixels using Photoshop Elements 8.0 (Adobe, San Jose, CA, USA) and saved in the GIF format (graphics interchange format). ImageJ software (1.44) with the NeuronJ plug-in (1.4.2) run on Windows 7 (Microsoft, Redmond, Washington, USA) (Meijering *et al.*, 2004) was used for the semiautomatic neurite tracing. Neurite lengths in pixels were measured, and the DAPI stained cells were manually counted. The total neurite length per image and neurite length divided by the number of cells possessing neurites were calculated.

Comments

Neurite tracing with NeuronJ allows to quantify neurite outgrowth from the microscopy images of cells. The method is, however, time-consuming and labour-intensive compared to the microplate reader measurements. It takes hours to get the same amount of data as received by minutes of reading in the fluorescence microplate reader. Additionally, the subjective error that might be present in the semiautomatic neurite tracing is eliminated in the fluorescence measurements in the plate reader.

Propidium iodide assay (Paper I)

Propidium iodide (PI) was applied to measure total DNA content and cell death during the process of neuronal differentiation of P19 cells. PI is a red fluorescent dye that enters the cells via a damaged cell membrane and binds to the double-stranded DNA (Dengler *et al.*, 1995). PI bound to DNA undergoes 20- to 30-fold fluorescence enhancement that is detected at excitation/emission wavelengths of 535/617 nm.

Cell samples were treated for 10 min with 0.2 % Triton X-100 to determine total DNA content during the process of neuronal differentiation in P19 cells. Non-treated cells were used to measure cell death during the neuronal differentiation. PI (10 µg/ml) was applied to the cells and incubated together with calcein-AM for 40-60 min. The cells were washed with Dulbecco's PBS and the fluorescence was measured in a fluorescence microplate reader with 544/620 nm excitation/emission filters.

Cell viability analyses

For cell viability analyses, the cells were plated in 96-well plates (optically clear for colorimetric assays, and black plates with clear bottoms for fluorometric assays). The cells were incubated with test compounds or vehicles at 37 °C, 5 % CO_2 unless otherwise stated.

Calcein-AM assay (Paper I, II, IV)

Calcein is a fluorescent dye used for the assessment of cell viability. Calcein-acetoxymethyl (AM) is a non-fluorescent derivative of calcein that easily permeates the cell membrane. Inside the cells, the intracellular esterases remove the AM group, and calcein emits a strong green fluorescence at excitation/emission maximum around 495/550 nm (Lichtenfels *et al.*, 1994; Roden *et al.*, 1999).

Calcein-AM dye (Molecular probes™, Thermo Fisher Scientific, Uppsala, Sweden) was reconstituted with DMSO and further diluted with PBS. The final concentration of DMSO in the assay was 0.01 %. The cells were washed with PBS and incubated with 1 µl calcein-AM for 1 h protected from light. Fluorescence was measured in a fluorescence microplate reader with 490/520 nm excitation/emission filters. Cells treated with 2 % Triton X-100 for 30 min served as controls for total cell death. Representative images of the samples were obtained using the fluorescence microscope.

Comments

Calcein has a relatively good retention time in living cells, at least 4 h, and a limited spontaneous leakage (Lichtenfels *et al.*, 1994). However, lysed cells that retain active esterases can convert calcein-AM to the fluorescent calcein that eventually is released into the surrounding media. Indeed, calcein can be detected in the supernatant hours after exposure of cells to calcein-AM to estimate the number of lysed cells in a fluorescence plate reader (Neri *et al.*, 2001). Due to the calcein production of lysed cells, the cytotoxicity might be underestimated when total calcein fluorescence is determined.

LDH release (Paper I, II, III, IV)

Lactate dehydrogenase (LDH) assay is a colorimetric method to measure cytotoxicity. LDH is an enzyme present in the cytosol of most cell types. LDH is released into the surrounding media when the cell is damaged and the plasma membrane is disrupted. LDH activity in the media increases proportionally to the number of lysed cells. LDH assay was performed using the LDH cytotoxicity detection kit obtained from Roche Diagnostics (Mannheim, Germany) according to the manufacturer's instructions. Aliquots of cell culture media were transferred to an optically clear 96-well flat bottom microtiter plate. The mixture of kit reagents was added to the samples, and the plate was incubated for 30 min at room temperature protected from light. The samples were measured spectrophotometrically at 490 nm with a reference wavelength of 650 nm. The total amount of released LDH was measured in cell samples incubated with 2 % Triton X-100 for 30 min at 37 °C, 5 % CO_2. The data was expressed as percentage of the LDH released by the Triton X-100 treatment.

Comments

Serum in media, including FBS, contains LDH and therefore might give high background readings in the LDH assay. To avoid this, cells should preferentially be maintained in serum-free or low-serum media for use in the assay, that was the case in our studies.

MTT reduction (Paper III, IV)

MTT reduction assay is a colorimetric method to measure cell viability. MTT is a yellow tetrazolium salt that is reduced in metabolically active cells to purple formazan crystals. The crystals are then solubilized and the absorbance is measured at 570 nm. The amount of formazan produced is proportional to the number of metabolically active cells present during MTT exposure (Mosmann, 1983). MTT reduction has been found in several subcellular fractions including mitochondrial, nuclear, microsomal and cytosolic fractions. The pyridine nucleotide cofactor NADH predominantly mediates cellular MTT reduction (Berridge & Tan, 1993; Berridge *et al.*, 2005).

Cell culture media were replaced with fresh media. MTT solution in PBS was added to the cell samples at a final concentration of 0.45 mg/ml. The cells were incubated for 3 h at 37 °C, 5 % CO_2 until the formazan crystals were formed. The crystals were solubilized with 0.01 M HCl/10 % SDS (sodium dodecyl sulfate) mixture overnight at room temperature protected from light. The absorbance was measured spectrophotometrically at 570 nm with a reference wavelength of 650 nm.

Comments
Formazan itself can damage cell membranes and reduce cell viability (Lu *et al.*, 2012).

PrestoBlue™ reduction (Paper II)

PrestoBlue™ is a resazurin-based reagent used for cell viability assessment (Invitrogen, 2012; Lall *et al.*, 2013). Resazurin is a water-soluble dye that is reduced by metabolically active cells to resorufin that can be measured fluorometrically with 540-570/580-610 nm excitation/emission filters, and colorimetrically at 570 nm and a reference wavelength of 600 nm (Invitrogen, 2012).

PrestoBlue™ (Thermo Fisher Scientific, Uppsala, Sweden) was added 1:10 to the cells and incubated for 30 min at 37 °C, 5 % CO_2. Fluorescence was measured in a fluorescent plate reader with 544/612 nm excitation/emission filters.

Comments

PrestoBlue™ reduction data is comparable to MTT reduction results (Invitrogen, 2012; Boncler *et al.*, 2014; Xu *et al.*, 2015). Advantages of using PrestoBlue over MTT include that it is faster, easier to perform, generally non-toxic to the cells at the recommended conditions and sensitive enough to monitor a low number of cells (less than 100 cells/well) (Invitrogen 2012; Boncler *et al.*, 2014).

Mitochondrial membrane potential (ΔΨm) analysis (Paper II, III, IV)

TMRE (tetramethylrhodamine ethyl ester) assay is a fluorometric assay that measures mitochondrial membrane potential. TMRE is a positively charged red-orange dye that permeates the cells and accumulates in the negatively charged active mitochondria. Depolarized mitochondria that have a less negative charge accumulate less TMRE (Perry *et al.*, 2011).

A positive control, the uncoupler of mitochondrial oxidative phosphorylation FCCP (5 μM) (carbonyl cyanide 4-[trifluoromethoxy]phenylhydrazone) was added to the cells for 10 min incubation at 37 °C, 5 % CO_2 prior to the addition of TMRE. The medium was changed and 500 nM TMRE was added to the cells for 30-45 min incubation at 37 °C, 5 % CO_2. The cells were washed once with Hanks' balanced salt solution (HBSS) with $CaCl_2$ and $MgCl_2$/0.2 % bovine serum albumin and fluorescence was measured in a fluorescence plate reader with 544/590 nm excitation/emission filters.

Reverse transcription PCR (Paper III)

Total RNA was extracted from P19 cells and P19 neurons using RNeasy mini kit (QIAGEN, Sollentuna, Sweden) and from the mouse brain (cerebrum) using miRNeasy mini Kit (QIAGEN, Sollentuna, Sweden) according to the

manufacturer's instructions. The RNA concentrations were measured in a NanoDrop Lite spectrophotometer (Thermo Fisher Scientific, Shanghai, P.R. China) at 260 nm. cDNA was synthesized using High Capacity cDNA Reverse Transcription kit (Applied Biosystems, Stockholm, Sweden). For the end-point PCR analyses, 4 ng/reaction of the cDNA template was used.

Primers sequences for SERT (127 bp) were 5´-TGCCTTTTATATCGCCTCCTAC-3´ (forward) and 5´-CAGTTGCCAGTGTTCCAAGA-3´ (reverse). The PCR program for sequence amplification consisted of the initial denaturation step, 3 min at 94 °C, followed by 35 cycles each of 45 sec at 94 °C (denaturation), 45 sec at 60 °C (annealing) and 60 sec at 72 °C (extension) and the final extension, 10 min at 72 °C. PCR products were separated with agarose gel electrophoresis on 1.2 % agarose gel stained with GelRed (Biotium, Hayward, CA, USA).

Real-time quantitative PCR (Paper III)

mRNA extraction from P19 cells and P19 neurons was performed using Dynabeads® mRNA Direct kit (Ambion, Life Technologies AS, Oslo, Norway). The cells were washed with PBS, lysed with the kit lysis buffer and stored at -80 °C. mRNA was extracted according to the manufacturer's instructions. mRNA (50 ng) was used to synthesize cDNA with High Capacity cDNA Reverse Transcription kit (Applied Biosystems, Stockholm, Sweden). Quantitative PCR (qPCR) reactions were run in Eco™ instrument and software (Illumina, Inc., San Diego, CA, USA). Each PCR sample contained cDNA (1.6 µl) and SYBR Green mix (KAPA SYBR® FAST qPCR Master Mix) in a total volume of 20 µl. The samples were run in duplicates. The program for amplification was: 10 min at 95 °C (initial denaturation), followed by 45 cycles of 10 sec at 95 °C (denaturation), 30 sec at 60 °C (annealing) and 15 sec at 72 °C (extension). For the product analyses, a melt curve was generated at the end of the PCR. Data were normalized to the mRNA expression of 60S ribosomal protein L19 (RPL19).

The primer sequences for SERT were 5′-GCTGATGATGTAAGGTCTTTCTCC-3′ (forward) and 5′-AGTCCAAGAGAGTTCATGGAAAG-3′ (reverse). The primer sequences for RPL19 were: 5′-TACTGCCAACGCTCGCAT-3′ (forward) and 5′-AACACATTCCCTTTGACCTTCA-3′ (reverse).

ELISA for serotonin transporter (Paper III)

ELISA kit for serotonin transporter (SERT) (mus musculus) (USCN Life Science Inc., Hubei, P.R. China) was used for detection of the protein SERT in P19 cells and P19 neurons. The assay was performed according to the manufacturer's instructions. Cell lysates were collected according to the following procedure. The cells were washed three times with ice-cold PBS, detached by scraping, collected, and centrifuged for 5 min, ~200 g, 4 °C. The pellets were diluted with 0.5 ml PBS, sonicated on ice, and centrifuged at 1500 g for 10 min at 4 °C. The supernatants were stored at -80 °C until use in the assay. The protein concentrations were determined with Pierce® BCA protein assay kit (Thermo Scientific, Rockford, IL, USA). In the ELISA, standards, blanks and protein samples (2.5 mg/ml) were incubated for 2 h at 37 °C with SERT-specific antibodies directed towards the C-terminal of the mouse SERT protein (the sequence from Arg461 to Val630) pre-coated on the microtiter plate. The liquid was removed from the plate, and the samples were incubated for 1 h at 37 °C with the biotin-conjugated detection antibodies specific to SERT. The plate was washed three times with the washing buffer, and incubated for 30 min at 37 °C with avidin conjugated to horseradish peroxidase (HRP). The plate was washed five times with the washing buffer, and the TMB substrate solution was added for 22 min incubation at 37 °C. The stop solution was added, and the absorbance was measured at 450 nm.

Western blot (paper III)

Cell lysates for Western blot analysis were collected according to the following protocol. The cells were washed twice with PBS, dislodged by scraping, collected, and centrifuged for 5 min at ~200 g, 4 °C. The pellets were lysed with RIPA buffer

containing protease inhibitor cocktail III (1:200), agitated for 30 min at 4 °C, sonicated on ice, and centrifuged for 5 min at 14 000 g, 4 °C. The supernatants were stored at -80 °C. The protein concentrations were determined with Pierce® BCA protein assay kit. The proteins (10 µg/sample) were separated by SDS-PAGE on Mini-PROTEAN® TGX™ Precast gels (BIO-RAD Laboratories, Inc., USA), and transferred on PVDF membranes. Non-specific binding was blocked by incubating the membranes in 5 % dried milk in tris-buffered saline, 0.1 % Tween 20 buffer (TBST) for 1 h under agitation. Primary rabbit monoclonal anti-monoamine oxidase A antibodies [EPR7101] (ab126751) (Abcam, Cambridge, UK) diluted 1:1000 were applied to the membranes overnight at 4 °C. The membranes were washed five times, 6 min per wash, with TBST buffer, and incubated for 1 h with secondary HRP-conjugated polyclonal goat anti-rabbit antibodies diluted 1:2000 (Dako, Glostrup, Denmark). The membranes were washed five times, 6 min per wash. The proteins bound to the antibodies were detected with chemiluminiscence using ClarityTM Western ECL Substrate. The images were obtained with the Image LabTM Software (BIO-RAD Laboratories, Inc., USA).

Uptake assay of [^{3}H]-5-HT in P19 neurons (Paper III)

The assay was a modification of the method described by Rudd *et al.*, 2005. The cells were plated in 12-well plates at a density of 1000 cells/mm^2 and differentiated for eight days in the serum-free medium. The plates were washed two times with warm (37 °C) uptake buffer (140 mM NaCl, 2 mM KCl, 1 mM $CaCl_2$, 1 mM $MgCl_2$, 5 mM D-glucose, 10 mM HEPES, pH 7.4). Uptake buffer containing 250 µM ascorbic acid, 10 µL pargyline and 0.1 % fatty acid free bovine serum albumin was added to the plates. The antioxidant ascorbic acid was used to prevent decomposition of [^{3}H]-5-HT (Hamblin *et al.*, 1987). The monoamine oxidase inhibitor pargyline was applied to prevent oxidative deamination of the serotonin taken up by the cells (Katz & Kimelberg, 1985). Bovine serum albumin (0.1 %) was used to reduce non-specific binding of [^{3}H]-5-HT to plastic. The wells were incubated with test compounds or vehicle for 10 min at 37 °C. To start the reaction, 100 nM [^{3}H]-5-HT was added for 30 min incubation at 37 °C. To terminate the

uptake, the plates were placed on ice and washed twice with an ice-cold uptake buffer. The samples were solubilized by incubation in 0.2 M NaOH for 15 min at 75 °C, and the aliquots were transferred to scintillation vials. The tritium content was determined by liquid scintillation spectroscopy with quench correction. Wells with medium alone were used to detect residual non-specific binding of [^{3}H]-5-HT to the wells.

Statistics

All statistical analyses were performed using the computer software GraphPad Prism 5, 6 or 7 for the Macintosh (GraphPad Software Inc., San Diego, CA, USA). P-values of < 0.05 were considered statistically significant.

In paper I, a two-tailed t-test was applied to identify differences in means between two data sets. In papers II, III and IV, one or two-way ANOVAs were undertaken and, upon significance, followed by Dunnett's or Bonferroni's *post hoc* tests. The one-way ANOVA (analysis of variance) is used to compare means of three or more samples. The two-way ANOVA examines effects of two different factors on a measured variable and an interaction effect of the factors.

Results

Fluorescence-based microplate reader assay for detection of neurite outgrowth in P19 neurons immunostained against βIII-tubulin (paper I)

Fluorescence of P19 neurons immunolabelled against the cytoskeletal neuron-specific protein βIII-tubulin was measured in a fluorescence microplate reader. The data was compared to the results of a semiautomatic neurite tracing in the fluorescence microscopy images of the cells that measured neurite length per image. On differentiation days 2-10, the time-dependent increase in fluorescence of anti-βIII-tubulin antibodies corresponded well to the increase in the total neurite length per image (Fig. 1). The increase in the βIII-tubulin fluorescence was not due to cell proliferation (paper I, Fig. 1E), and it primarily came from the neurites. Since the βIII-tubulin microplate reader assay is fast compared to the neurite tracing method, it is suitable for detection of neurite outgrowth in high-throughput neurotoxicity testing of chemicals.

The βIII-tubulin microplate reader assay was evaluated for testing of chemical-induced effects on neurite outgrowth. The assay was compared to the fluorescence-based calcein-AM cell viability assay (Fig. 2). The βIII-tubulin assay was more sensitive than the calcein-AM assay to detect toxicity of the compounds toxic to neurites: nocodazole, methylmercury and okadaic acid (Solomon, 1980; Castoldi *et al.*, 2001; Chiou & Westhead, 1992). For nocodazole (1 nM), methylmercury (50 nM) and okadaic acid (1 nM), fluorescence of βIII-tubulin vs. calcein expressed as percentage of untreated cells was 86 % (± 1.7) vs. 106 % (± 2.1); 83 % (± 6.2) vs. 107 % (± 5.8) and 59 % (± 6.6) vs. 86 % (± 6.5), respectively (Fig. 2A, B & C). However, for dimethyl sulfoxide and glutamate, there were no significant differences in the observed readouts between the two assays (Fig. 2D & E). For clomipramine (30 µM), calcein fluorescence decreased to 19 % (± 3.0) of untreated cells compared to βIII-tubulin fluorescence that was 62 % (± 14) of untreated cells (Fig. 2F).

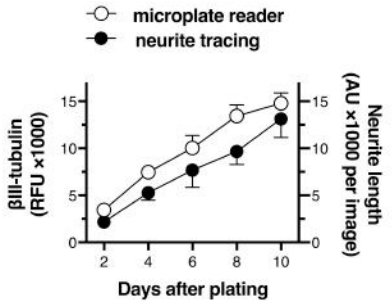

Fig 1. Assessment of time-dependent neurite outgrowth in P19 neurons immunostained against βIII-tubulin. P19 cells were neuronally differentiated for 2-10 days in the serum-free media. White circles show relative fluorescence units (RFU) (left y-axis) of anti-βIII-tubulin antibodies measured in a fluorescence microplate reader. Black circles show arbitrary units (AU) (right y-axis) of semiautomatic neurite tracing in fluorescence microscopy images using the ImageJ software with the NeuronJ plug-in. Data are means ± s.e.m. of 3-4 independent experiments.

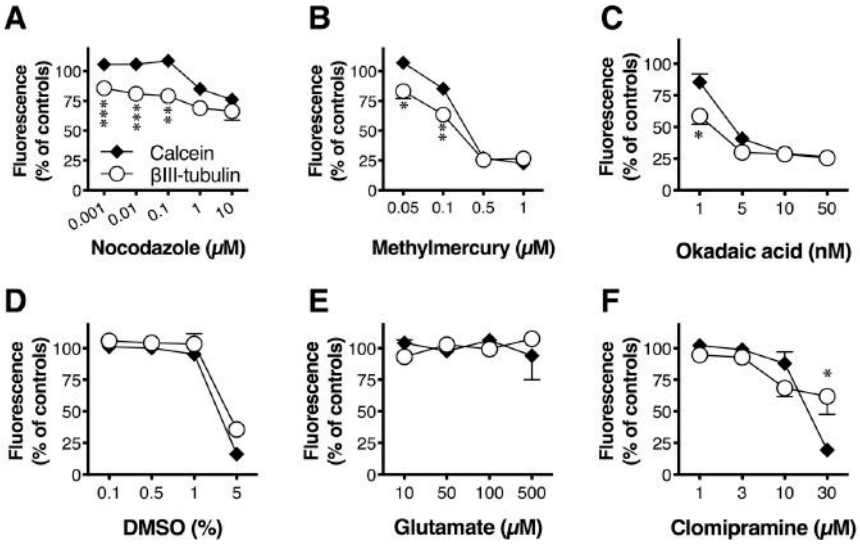

Fig. 2. Concentration-dependent effects of nocodazole, methylmercury, okadaic acid, DMSO, glutamate and clomipramine on fluorescence of anti-βIII-tubulin antibodies and calcein in P19 neurons. The cells were exposed to the test compounds on day 6 in the serum-free media for 48 h (24 h for nocodazole). The cells were immunostained against βIII-tubulin or treated with calcein-AM. Fluorescence of anti-βIII-tubulin antibodies (white circles) and calcein (black diamonds) was measured in a fluorescence microplate reader. Data are means ± s.e.m. of 3-5 independent experiments, and expressed as percentage of untreated cells. Statistical analysis was performed using two-tailed t-test: *$p < 0.05$, **$p < 0.01$ and ***$p < 0.001$ (comparisons between fluorescence values of anti-βIII-tubulin antibodies and calcein at each concentration).

The LDH assay was also used in the study as a readout of cell damage. Exposure of P19 neurons to 100 μM glutamate and 10 μM clomipramine on day 6 in the serum-free media for 48 h resulted in small but significant toxic effects that were 11 % (± 1.5) and 15 % (± 0.5) of total cell death, respectively (paper I, Fig. 3). LDH leakage might reflect effects of these chemicals on cell bodies rather than on neurite outgrowth that the βIII-tubulin microplate reader assay primarily measures.

The data suggest that the βIII-tubulin microplate reader assay is useful for detection of chemical-induced changes in neurite outgrowth and might be used in addition to other methods for toxicological assessment of chemicals.

Neurons derived from mouse P19, rat PC12 and human SH-SY5Y cells in neurotoxicity assessment of methylmercury, okadaic acid and acrylamide (paper II)

P19 neurons, retinoic acid-differentiated SH-SY5Y cells and NGF-stimulated PC12 cells were compared for detection of toxic effects of methylmercury (MeHg), okadaic acid and acrylamide. The cells were exposed to the compounds on day 6 in the differentiation medium for 48 h. In P19 neurons, 0.5 μM MeHg, 10 nM okadaic acid and 1000 μM acrylamide significantly decreased calcein fluorescence to 77 % (± 9.8), 75 % (± 6.5) and 87 % (± 3.1) of control cells, respectively (means ± s.e.m.) (Fig. 3). MeHg and okadaic acid-treated cells were compared to DMSO vehicle-treated cells. The final concentration of DMSO in the samples was 0.1 %. Cells exposed to acrylamide were compared to untreated cells. In SH-SY5Y cells, only MeHg (1 μM) reduced calcein fluorescence to 76 % (± 11) of control, and in PC12 cells, none of the tested compounds significantly decreased calcein fluorescence (Fig. 3).

In P19 neurons and differentiated SH-SY5Y cells, the involvement of glutathione (GSH) in MeHg toxicity was examined using PrestoBlue as readout. In both cell models, extracellular GSH protected against MeHg toxicity (Fig. 4).

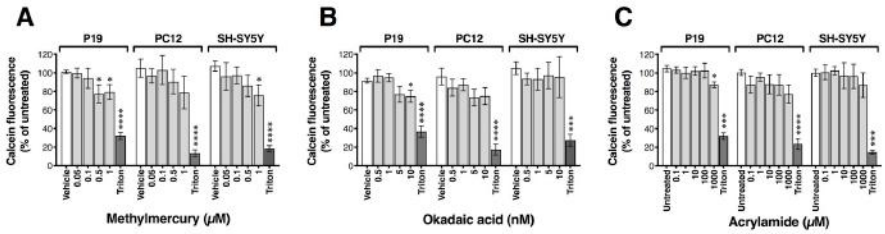

Fig. 3. Concentration-dependent effects of methylmercury, okadaic acid and acrylamide on calcein fluorescence in differentiated P19, PC12 and SH-SY5Y cells. The cells were exposed to (A) methylmercury, (B) okadaic acid and (C) acrylamide for 48 h on day 6 in the differentiation media. The data are means ± s.e.m. of n = 4-6, and expressed as percentage of 0.1 % DMSO vehicle-treated cells, or untreated cells for acrylamide. Statistical analyses were performed using repeated measures one-way ANOVA with *post hoc* Dunnett's multiple comparisons test for each compound and cell line compared to respective controls (*p < 0.05, ***p < 0.001, ****p < 0.0001).

In P19 neurons, PrestoBlue reduction upon exposure to 1 μM MeHg was 35 % (± 2.4) and, in combination with 1 mM GSH, 65 % (± 7.1) of untreated controls (means ± s.e.m.) (Fig. 4). Buthionine sulfoximine (BSO) (100 μM), a potent inhibitor of GSH synthesis, combined with 1 μM MeHg decreased cellular redox potential to 17 % (± 1.9) of untreated controls.

In differentiated SH-SY5Y cells, exposure to 1 μM MeHg decreased cellular redox potential to 47 % (± 8.0) of untreated controls. Upon exposure to both MeHg and GSH, PrestoBlue reduction was 103 % (± 5.6) of untreated controls. BSO (100 μM) together with 1 μM MeHg decreased cellular redox potential to 22 % (± 6.8) of untreated cells (Fig. 4).

The effects of MeHg (1 μM) alone and in combination with GSH (1 mM) or BSO (100 μM) on mitochondrial membrane potential (ΔΨm) were examined in P19 neurons and retinoic acid-differentiated SH-SY5Y cells (Fig. 5). In P19 neurons, exposure to MeHg, MeHg+GSH and MeHg+BSO, reduced ΔΨm to 59 % (± 2.5), 86 % (± 4.8) and 45 % (± 2.1) of untreated cells, respectively (means ± s.e.m.) (Fig. 5). In differentiated SH-SY5Y cells, MeHg, MeHg+GSH and MeHg+BSO exposure reduced ΔΨm to 60 % (± 4.2), 89 % (± 7.8) and 58 % (± 4.7) of untreated cells, respectively (Fig. 5).

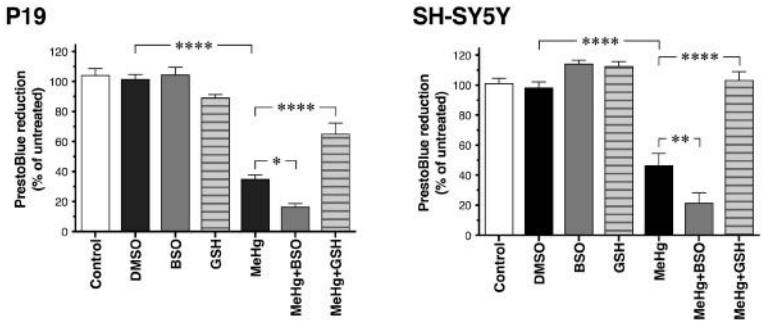

Fig. 4. Effects of MeHg, GSH and BSO on PrestoBlue reduction in neurons derived from P19 and SH-SY5Y cells. The cells were pretreated with 100 μM BSO for 17 h or with 1 mM GSH for 1 h and then exposed to 1 μM MeHg for 24 h on day 6 of differentiation. Cell viability was assessed with PrestoBlue assay. Data are means ± s.e.m. of n = 6, and expressed as percentage of untreated cells. One-way ANOVAs were performed with *post hoc* Bonferroni's multiple comparisons test (****$p < 0.0001$ for MeHg vs. 0.1 % DMSO vehicle-treated cells, and for MeHg vs. MeHg+GSH for both cell types; *$p < 0.05$ for MeHg vs. MeHg+BSO for P19 neurons; **$p < 0.01$ for MeHg vs. MeHg+BSO for retinoic acid-differentiated SH-SY5Y cells).

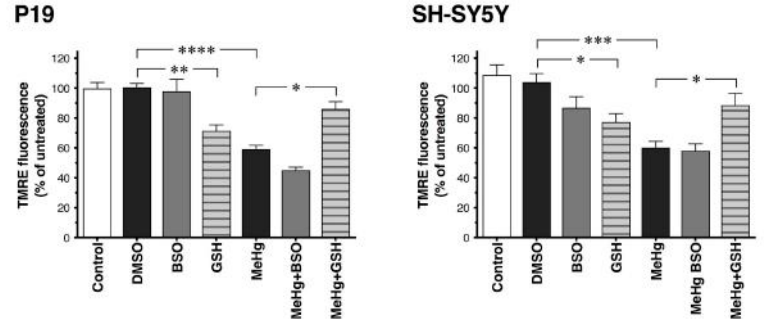

Fig. 5. Effects of MeHg, GSH and BSO on TMRE fluorescence in neurons derived from P19 and SH-SY5Y cells. The cells were treated with 100 μM BSO for 17 h or with 1 mM GSH for 1 h and then exposed to 1 μM MeHg for 24 h on day 6 in the differentiation media. Mitochondrial membrane potential was measured with TMRE assay. Data are means ± s.e.m. of n = 6, and expressed as percentage of untreated cells. One-way ANOVAs with *post hoc* Bonferroni's multiple comparisons test showed for P19 neurons: ****$p < 0.001$ for MeHg vs. 0.1 % DMSO vehicle-treated cells, **$p < 0.01$ for GSH vs. vehicle-treated cells, *$p < 0.05$ for MeHg vs. MeHg+GSH-treated cells; for SH-SY5Y cells: ***$p < 0.001$ for MeHg vs. vehicle-treated cells, *$p < 0.05$ for GSH vs. vehicle-treated cells and for MeHg vs. MeHg+GSH-treated cells.

P19 neurons were the most sensitive of the three cell models to detect toxicity of methylmercury, okadaic acid and acrylamide under the examined conditions. For the detection of mechanisms of toxicity of MeHg, P19 neurons were at least as sensitive as differentiated SH-SY5Y cells. In both cell models, MeHg decreased cellular redox potential and mitochondrial membrane potential, and MeHg toxicity was attenuated by GSH. In conclusion, P19 neurons might be used for neurotoxicity assessment of chemicals in conjunction with other *in vitro* cellular models.

Neurotoxicity of MDMA in P19 neurons (paper III) and differentiated SH-SY5Y cells

MDMA produced time-, concentration- and temperature-dependent toxicity in P19 neurons treated on day 7 in the serum-free media as assessed using MTT reduction assay (Fig. 6). Upon exposure to 1 mM MDMA for 24, 48 and 72 h, MTT reduction was 76 % (± 6.3), 54 % (± 11.6) and 40 % (± 4.1) of untreated cells, respectively (means ± s.e.m.). After 24 h of exposure to 1 mM MDMA at 40 and 42 °C, MTT reduction was 67 % (± 3.7) and 5 % (± 1.8) of untreated cells, respectively (Fig. 6).

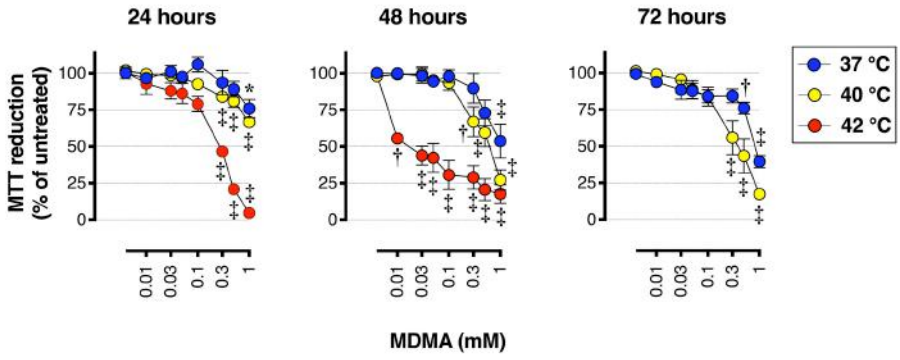

Fig. 6. Time-, concentration- and temperature-dependent effects of MDMA on MTT reduction in P19 neurons. The cells were exposed to MDMA on day 7 in the serum-free media for 24, 48 and 72 h at the temperatures 37, 40 and 42 °C. Cell viability was assessed with MTT reduction assay. Data are means ± s.e.m. of n = 4-5, and expressed as percentage of untreated cells. One-way ANOVAs were performed with *post hoc* Dunnett's multiple comparisons test compared to the corresponding controls (*$p < 0.05$, †$p < 0.01$, ‡$p < 0.001$).

The involvement of the proteins SERT and MAO in the toxicity of MDMA was examined. If MDMA produced its neurotoxic effects secondary to blockade of MAO and/or SERT (see Introduction), then it would be expected that compounds inhibiting these targets would produce similar neurotoxic effects in the cells. However, the MAO-A inhibitor clorgyline, the MAO-B inhibitor deprenyl and the SERT inhibitor fluoxetine did not *per se* or in combination mimic the toxic effects of MDMA assessed with MTT reduction assay (paper III, Table 1).

Among other potential causes of MDMA toxicity in P19 neurons, oxidative stress and changes in the mitochondrial membrane potential were investigated. Oxidative stress was probably not the primary cause of the MDMA toxicity since the antioxidants N-acetyl-L-cysteine and α-tocopherol did not reduce toxic effects of MDMA in P19 neurons (paper III, Fig. 4). MDMA did not affect the mitochondrial membrane potential in the cells (paper III, Fig. 5).

In contrast to the robust effects upon P19 neurons, MDMA did not affect the cell viability of retinoic acid-differentiated SH-SY5Y cells under the conditions examined and with MTT as the readout (Fig. 7).

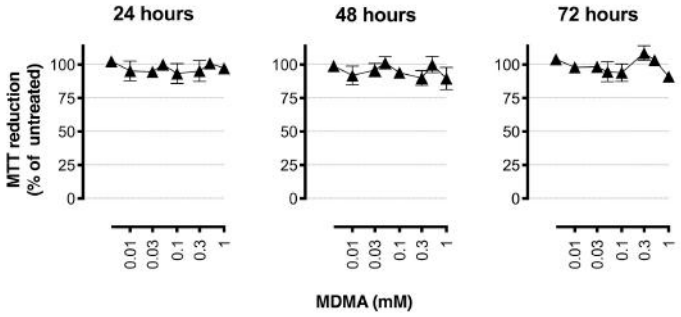

Fig. 7. Time- and concentration-dependent effects of MDMA on MTT reduction in retinoic acid-differentiated SH-SY5Y cells. The cells were exposed to MDMA for 24, 48 and 72 h at 37 °C, 5 % CO_2 on day 3 in the differentiation medium. Cell viability was assessed with MTT reduction assay. The data are means ± s.e.m. of n = 3. One-way ANOVAs showed no significant differences between the effects of different concentrations of MDMA on MTT reduction.

Toxicity of piperazine derivatives in P19 neurons, retinoic acid-differentiated SH-SY5Y cells and human epithelial colorectal adenocarcinoma Caco-2 cells (paper IV)

The piperazine derivatives BZP, TFMPP, MeOPP and pFPP were assessed for cytotoxicity in P19 neurons and retinoic acid-differentiated SH-SY5Y cells, and compared to MDMA "ecstasy". BZP and TFMPP were additionaly tested in human epithelial colorectal adenocarcinoma Caco-2 cells. The cells were exposed to the compounds for 24 h at the concentrations up to 1 mM. In P19 neurons, each of the examined piperazine derivatives decreased cell viability in at least one of the assays used (calcein-AM, LDH release or MTT reduction). In differentiated SH-SY5Y cells, only TFMPP reduced cell viability. In Caco-2 cells, both BZP and TFMPP were cytotoxic. TFMPP was the most toxic among the tested compounds.

MDMA, however, did not affect cell viability in P19 neurons in this study that was different from the results in paper II. In the present study, MTT reduction, upon exposure to 1000 μM MDMA for 24 h on day 7 in the serum-free media, was 77 % (± 7.7) of untreated cells vs. 97 % (± 3.6) in the untreated controls (means ± s.e.m, n = 5). At the same conditions in paper II, MTT reduction in MDMA-treated vs. untreated cells was 66 % (± 4.6) vs. 98 % (± 2.7), $p < 0.01$ (paper II, Table 1), and 76 % (± 6.3) vs. 100 % (± 3.9), $p < 0.05$ (paper II, Fig. 2), respectively (means ± s.e.m, n = 4 for each set of experiments). The lack of a significant effect of MDMA on MTT reduction in P19 neurons in the present study might be due to the large standard error of the mean in MDMA-treated and untreated cell samples. The experimental procedure of medium changing before addition of MTT to the cells affects variability between the samples. P19 neurons that are not strongly attached to the wells migh be rinsed off the wells if the media is changed fast enough. For some of the experiments, it migh be the case, that could explain the large variability between the samples, and therefore the non-significant effect of MDMA in the present study.

In P19 neurons exposed to 1000 µM MeOPP, 500 µM pFPP and 500 µM TFMPP, MTT reduction was 63 % (± 8.1), 68 % (± 3.3) and 2.2 % (± 0.9) of untreated cells, respectively (Fig. 8). BZP did not significantly affect MTT reduction, but decreased cell viability in the calcein-AM and the LDH assays (paper IV, Fig.1). In differentiated SH-SY5Y cells, MTT reduction upon exposure to 500 µM TFMPP was 3.0 % (± 1.8) of untreated controls. In Caco-2 cells treated with 500 µM BZP and TFMPP, MTT reduction was 83 % (± 4.9) and 4.4 % (± 1.3) of untreated cells, respectively (Fig. 8).

In P19 neurons, only TFMPP among the examined piperazine derivatives, decreased the mitochondrial membrane potential (ΔΨm). TFMPP reduced the ΔΨm before changes in the extracellular LDH levels were observed (Fig. 9). After 0.5, 2 and 6 h of exposure to 500 µM TFMPP, ΔΨm was 28 % (± 2.6), 27 % (± 0.6) and 29 % (± 6.1) of the vehicle-treated cells, respectively. LDH release for the same time points was 5.8 % (± 0.6), 25 % (± 2.2) and 40 % (± 2.3) of total cell death (cell treated with 2 % Triton X-100) (Fig. 9).

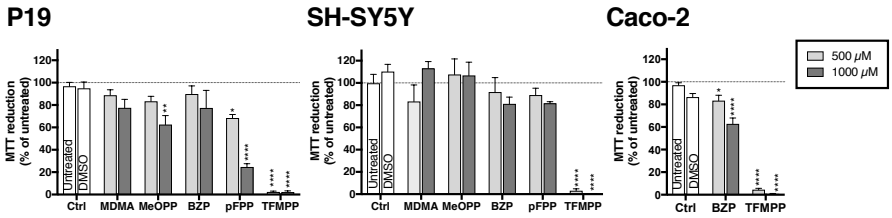

Fig. 8. Effects of MDMA and piperazine derivatives on MTT reduction in P19 neurons, retinoic acid-differentiated SH-SY5Y cells and Caco-2 cells. The cells were exposed to the test compounds for 24 h. P19 and SH-SY5Y cells were treated on days 7 and 3 in the differentiation media, respectively. The data are means ± s.e.m. of n = 5 for P19, n = 4 for SH-SY5Y and n = 6 for Caco-2 cells. The data are expressed as percentage of untreated cells. One-way ANOVAs were undertaken with *post hoc* Bonferroni's multiple comparisons test for the treated cells vs. untreated controls, and for TFMPP vs. 0.5 % DMSO vehicle-treated cells (*$p < 0.05$, **$p < 0.01$, ****$p < 0.0001$).

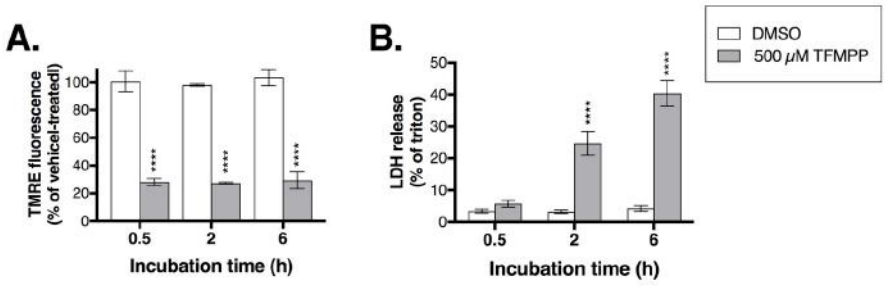

Fig. 9. Time-dependent effects of TFMPP on TMRE fluorescence and LDH release in P19 neurons. The cells were exposed to 500 μM TFMPP or 0.5 % DMSO vehicle on day 7 in the serum-free media for 0.5, 2 and 6 h. (A) Mitochondrial membrane potential was assessed with TMRE assay. (B) Cell membrane integrity was measured with LDH assay. For TMRE assay, the data are expressed as percentage of vehicle-treated cells. For LDH assay, the data are expressed are percentage of total cell death (cells lysed with 2 % Triton X-100). Data are means ± s.e.m. of n = 3. Two-way ANOVAs showed significant effects of treatment for both assays ($p < 0.0001$). For LDH assay, significant effects of time and the interaction term time x treatment ($p < 0.0001$) were detected. *Post hoc* Bonferroni's multiple comparisons test was performed for TFMPP-treated vs. corresponding vehicle-treated cells (****$p < 0.0001$).

Discussion

Overall comments

The studies in this thesis provide novel information about neurons derived from mouse embryonal carcinoma P19 cells as a model for neurotoxicity assessment of chemicals. The cell model detected toxicity of different chemicals known to be neurotoxic including MeHg, acrylamide, okadaic acid, MDMA and the piperazine-derived designer drugs. For some of the compounds, P19 neurons were compared to other commonly used cell models for neurotoxicity studies: retinoic acid-differentiated human SH-SY5Y cells and NGF-stimulated rat PC12 cells. In general, the chemicals at the examined conditions were more often toxic to P19 neurons than to the two other cell models. Mechanisms of toxicity for some of the chemicals were investigated in P19 neurons. MeHg and the piperazine derivative TFMPP produced loss of mitochondrial membrane potential in P19 neurons, the effect also observed in other cell types such as the hippocampal neuronal cell line HT22 for MeHg, and the rat cardiac cell line H9c2 for TFMPP (Tofighi *et al.*, 2011; Arbo *et al.*, 2014). MDMA was toxic to P19 neurons, although this toxicity was not mediated by SERT and MAO, in contrast to the situation in rat brain (Fitzgerald & Reid, 1990; Leonardi & Azmitia, 1994).

Chemical-induced effects on neurite outgrowth, an important parameter in neurotoxicity testing, were detected in P19 neurons by measuring fluorescence of the cells immunostained against the neuron-specific cytoskeletal protein βIII-tubulin. The method was fast with a reasonable capacity, and therefore could be applied for screening of chemicals for neurotoxicity in addition to other methods. The findings presented here, showed that P19 neurons is a useful *in vitro* cellular model for screening of chemicals for potential neurotoxicity as well as for studies on mechanisms of toxicity. The model, of course, has its limitations. It is of mouse origin, and chemical-induced toxicity might differ between species. For example, MDMA destroys serotonin nerve terminals in rat brain (Battaglia *et al.*, 1987), while in mouse brain, it produces dopaminergic and/or serotonergic toxicity depending on

the mouse strain and the investigated brain region (O'Callaghan & Miller, 1994; Zhang *et al.*, 2006). In P19 neurons, the non-serotonergic nature of MDMA toxicity may thus partly depend on the mouse origin of the model. The other disadvantage of *in vitro* cellular models in general is that the models lack the complexity that animal models provide, and therefore it is difficult to extrapolate results to animals and humans. On the other hand, *in vitro* cellular models, due to their simplicity, are useful for toxicity screening of chemicals for prioritizing them for further toxicological evaluations *in vivo*.

Assessment of chemical-induced effects on neurite outgrowth in cells immunostained against βIII-tubulin

Neurite outgrowth is an important parameter in neurotoxicity assessment of chemicals (Radio & Mundy, 2008) since some compounds might disrupt neuronal development and cause cognitive impairments (Grandjean *et al.*, 1997; Jaako-Movits *et al.*, 2005). Automatic measurements of neurite outgrowth require expensive equipment and special software that limits the usage of the technique. On the other hand, semiautomatic neurite tracing in microscope images of cells using the free computer software ImageJ with the NeuronJ plug-in takes hours to perform. In paper I, we used rather inexpensive laboratory equipment, a fluorescence microplate reader for assessment of neurite outgrowth. P19 neurons were immunostained against the protein βIII-tubulin at days 2-10 of neuronal differentiation and fluorescence of the samples was detected in a fluorescence microplate reader. The data corresponded well to the data observed with the semiautomatic tracing of neurites. The fluorescence microplate reader method is fast and therefore suitable for high-throughput screening of chemicals for potential toxic effects on neurite outgrowth.

The disadvantage of the βIII-tubulin fluorescence microplate reader method compared to neurite tracing methods is that the measured fluorescence comes from both cell bodies and neurites. In the neurite tracing methods, cell bodies are excluded from calculations and only neurites are measured. The microplate reader

data is therefore somewhat less accurate, but as we showed in paper I, fully applicable for the measurements of neurite outgrowth in P19 neurons. In P19 neurons that are postmitotic, have small cell bodies and an extensive neurite network, the βIII-tubulin fluorescence mainly comes from the neurite extensions.

In retinoic acid-treated SH-SY5Y cells, neurite outgrowth was assessed with the βIII-tubulin microplate reader assay in paper II. The cells continued to proliferate during the differentiation process, and therefore, the assay was less accurate for detection of neurite development in this model compared to P19 neurons. In SH-SY5Y cells, the fluorescence of anti-βIII-tubulin antibodies increased partly due to an increased number of cells as the differentiation process proceeded. NGF-stimulated PC12 cells were also investigated in paper II. However, less number of the cells generated neurites compared to the differentiated P19 and SH-SY5Y cells, and the βIII-tubulin fluorescence was mainly generated from the cells bodies. Therefore, the βIII-tubulin fluorescence reader method was less accurate in NGF-treated PC12 cells for detecting changes in neurite outgrowth than in P19 neurons. Thus, it can be concluded that the βIII-tubulin fluorescence microplate reader method is useful for postmitotic cells that have an extensive neuronal network such as P19 neurons.

In P19 neurons, the βIII-tubulin fluorescence microplate reader assay detected toxicity of the chemicals toxic to neurites (nocodazole, MeHg and okadaic acid) at lower concentrations than the calcein-AM assay (Solomon, 1980; Castoldi *et al.*, 2001; Chiou & Westhead., 1992). The βIII-tubulin fluorescence microplate reader assay was, however, less sensitive to detect cytotoxicity of clomipramine and glutamate compared to the LDH assay. The latter assay might reflect toxicity of these chemicals to the cell bodies rather than changes in neurite outgrowth. In consequence, the βIII-tubulin microplate reader is a useful method for measuring chemical-induced effects on neurite outgrowth, but it should be used together with other assays for neurotoxicity assessment.

Neurotoxicity assessment of MeHg, okadaic acid and acrylamide in neurons derived from mouse P19, human SH-SY5Y and rat PC12 cells

As described in the Introduction, several *in vitro* cellular models have been used for toxicological evaluations of chemical. It is important to have various cellular models for neurotoxicity studies since the response to chemicals differs between different cell types (Wilson *et al.*, 2014). In paper II, we compared neurons derived from P19, SH-SY5Y and PC12 cells for the detection of toxicity of the known neurotoxic compounds: MeHg, okadaic acid and acrylamide (Fujimura *et al.*, 2016; Das & Miller, 2012; Attoff *et al.*, 2016). In P19 neurons, all three compounds were cytotoxic at the examined conditions, while in differentiated SH-SY5Y and PC12 cells, one and none of the chemicals decreased cell viability, respectively. MeHg produced toxicity in both P19 neurons and differentiated SH-SY5Y cells that was attenuated by the antioxidant GSH. Protective effects of GSH on MeHg toxicity had been observed in neuronal cell cultures such as human fetal neurons, astrocytes and SH-SY5Y cells (Sanfeliu *et al.*, 2001). In our study, MeHg also induced loss of mitochondrial membrane potential in P19 neurons and differentiated SH-SY5Y cells that is a known mechanism of MeHg toxicity (Tofighi *et al.*, 2011). In conclusion, P19 neurons were a most sensitive model compared to differentiated PC12 and SH-SY5Y cells to detect toxicity of MeHg, okadaic acid and acrylamide at the examined conditions. The model was at least as sensitive as retinoic acid-differentiated SH-SY5Y cells for detection of the mechanisms of MeHg toxicity.

Toxicity of drugs of abuse in P19 neurons and retinoic acid-differentiated SH-SY5Y cells

Substance abuse for recreational purposes is a growing problem especially among young adults in the global society. The availability of novel psychoactive substances with unknown toxic effects is increasing, putting the consumers at risk of getting harmed (Zawilska, 2015). It is important to test recreational substances for neurotoxic effects and to inform society about them. Cellular models provide opportunity to rapidly assess chemicals for toxic effects, but also to investigate

mechanisms of toxicity on the cellular level. In paper III, we investigated mechanisms of toxicity of the well-known drug of abuse MDMA "ecstasy" in P19 neurons. Since MDMA toxicity is species-dependent (Logan *et al.*, 1988) and very few studies have been performed on neuronal cell models from mice (Meamar *et al.*, 2010; Meamar *et al.*, 2012) our study adds valuable information on this topic.

MDMA produced time-, concentration- and temperature-dependent toxicity in P19 neurons. The toxicity did not involve inhibition of the proteins SERT and MAO that are known targets of MDMA (Fitzgerald & Reid, 1990; Leonardi & Azmitia, 1994). Other mechanisms of MDMA toxicity such as oxidative stress and mitochondrial dysfunction (Colado *et al.*, 1997; Capela *et al.*, 2013) were not detected in P19 neurons. The mechanistic data in our study was mostly negative, but still valuable since it ruled out some of the possible mechanisms of MDMA toxicity in P19 neurons.

In paper IV, the piperazine-derived designer drugs BZP, TFMPP, MeOPP and pFPP were assessed for toxicity in P19 neurons and retinoic acid-differentiated SH-SY5Y cells. In P19 neurons, all tested compounds decreased cell viability at the examined conditions, but in differentiated SH-SY5Y cells, only TFMPP showed effects upon this parameter. Additionally, we investigated the toxicity of BZP and TFMPP in human epithelial colorectal adenocarcinoma Caco-2 cells to examine their effects in a non-neuronal cell line. Both compounds were toxic in Caco-2 cells. TFMPP was the most toxic compound among the tested piperazine derivatives that was also the case in the rat cardiomyoblast H9c2 cells (Arbo *et al.*, 2014) and retinoic acid-differentiated SH-SY5Y cells (Arbo *et al.*, 2016). In P19 neurons, TFMPP caused loss of mitochondrial membrane potential ($\Delta\Psi m$), while BZP, MeOPP and pFPP did not affects $\Delta\Psi m$. Effects of the piperazine designer drugs on $\Delta\Psi m$ differ between different cell types. For example, TFMPP decreased $\Delta\Psi m$ in a rat cardiac cell line (Arbo *et al.*, 2014) and in rat primary hepatocytes (Dias da Silva *et al.*, 2017), but in retinoic acid-differentiated SH-SY5Y cells, it hyperpolarized mitochondria (Arbo *et al.*, 2016). Our study showed that P19 neurons detected cytotoxicity of the examined

piperazine-derived designer drugs, and identified one of the mechanisms of TFMPP toxicity that was loss of mitochondrial membrane potential.

In conclusion, P19 neurons is a robust and simple model for assessment of chemical-induced neurotoxicity. It might be used in conjunction to other cellular models for prioritizing chemicals for further toxicological evaluations *in vivo.*

Future perspectives

The present studies lay the groundwork for future research. Possible avenues to explore include:

- To assess other types of known neurotoxic chemicals for toxicity in P19 neurons to validate further the model for neurotoxicity testing.

- To compare chemical-induced toxicity in mouse P19 neurons to human neuronal cell models, for example human induced pluripotent cells reprogrammed to neuronal cells.

- To investigate chemical-induced biochemical perturbations leading to neurotoxicity in cells. These include, but are not limited to, modulations of intracellular Ca^{2+} levels, formation of reactive oxygen and nitrogen species, GSH/GSGG ratio and DNA damage.

- To examine which forms of cell death are induced by chemicals i.e. apoptosis and/or necrosis.

Conclusions

- Fluorescence measurement of P19 neurons immunostained against the protein βIII-tubulin in a fluorescence microplate reader is a useful method to assess chemical-induced changes on neurite outgrowth.

- P19 neurons are more sensitive to detect cytotoxicity of MeHg, okadaic acid and acrylamide than retinoic acid-differentiated SH-SY5Y cells and NGF-treated PC12 cells. P19 neurons are at least as sensitive as differentiated SH-SY5Y cells to detect the protective effects of extracellular GSH on MeHg toxicity and the loss of mitochondrial membrane potential produced by MeHg.

- MDMA produces time-, concentration- and temperature-dependent toxicity in P19 neurons. The mechanisms of MDMA toxicity do not involve inhibition of the proteins SERT and MAO, oxidative stress or loss of mitochondrial membrane potential.

- The piperazine-derived designer drugs BZP, TFMPP, MeOPP and pFPP are toxic to P19 neurons. The most cytotoxic compound among these is TFMPP and its mechanism of action in P19 neurons includes loss of mitochondrial membrane potential.

Acknowledgements

I would like to express my gratitude to everyone who has contributed to this work in one way or another. Without your help and support it would not have been possible for me to complete it.

My supervisor **Stig Jacobsson.** Thank you for giving me the opportunity to do my PhD at the department. Thank you for introducing me to the field of toxicology that I found very interesting, and for constantly challenging me to gain new knowledge. I have learnt a lot from this journey, not only about the research, but also about myself.

Special thanks to my co-supervisor **Christopher Fowler** for giving me fast feedback on my writing and valuable ideas for some of my experiments. I greatly appreciate all the work you have done to help me finish my thesis. You are a true inspiration!

Gunnar Tiger and **Olov Nilsson,** thank you for being such good teachers in the subject of Pharmacology. I found the field interesting when I was a student and therefore applied for a PhD at the department.

Emmelie Björklund, Jessica Karlsson and **Linda Gabrielsson,** former and current PhD students, thank you for the good times in and out of the lab. I have enjoyed sharing the work space with you, discussing problems in the lab and talking about small and big things in life. **Emmelie**, good luck with your carrier as a medical doctor! **Jessica**, I appreciate your support in any issues during my PhD journey. I always knew I could rely on you at any time. It was nice having you as my roommate for such a long time! **Linda**, thank you for being my latest roommate and for all the talks we have had. Thanks for all the fantastic desserts you have made! Girls, wish you all the best in finishing your theses!

I would also like to thank former post docs **Maria Luisa Rojo, Antonio Rodriguez-Gaztelumendi, Linus Plym Forshell, Mariateresa Cipriano** and **Sanaz Hashemian**. It was such a pleasure to have you in the department! Thank you for all the laughs and interesting discussions! I enjoyed the international feeling you brought to the department! Special thanks to the current postdoc **Mireille Al Houayek**. You know so much about a lot of things in research and have always been helpful with any questions I have had. Thank you for being a great friend and colleague! I wish you all the best in your academic carrier!

Eva Hallin and **Mona Svensson,** thank you for all the practical support in the lab as well as for sharing the ups and downs of my research. You have been very helpful with ordering things for the lab and a great help with any practical issues. **Mona**, thank you for finding spelling mistakes in my thesis! **Agneta Valleskog**, thank you for the excellent administrative support and for always finding time to answer any administrative questions no matter how busy you have been. You have contributed a lot to the department not only with the enormous amount of work you do, but also with your great personality!

I want to thank some friends outside the lab that have made my PhD time more enjoyable. **Svetlana**, thank you for always being positive and having so much energy. It is inspiring! **Elisabet,** thank you for staying curious about my PhD even after you have left Umeå and for encouraging me to reach the goals on this journey. **Bernard**, thank you for the coffee breaks and the discussions throughout my PhD and about the next steps in our careers.

I want to thank Erik's family, his mother **Ingalill,** father **Håkan**, sisters **Maja** and **Greta,** and grandparents **Inga-Britt** and **Ingvar** for all the great weekends and lovely dinners in Junsele and Umeå. I am happy to have all of you in my life!

My father **Oleg,** thank you for giving me the opportunity to study in Sweden. This work would not exist if I did not get a degree in Biotechnology in Umeå in the first place.

I would like to give special thanks to my mother **Marina**, brother **Stas** and grandmother **Maja** for always being there for me and supporting me no matter where I was in my life. I wish we lived closer to each other than we do, but I know I can always call and talk to you about anything. I love you!

Thank you so much, my fiancé **Erik.** You mean everything to me, and your support during my PhD time has been enormous! Thank you for encouraging me and giving me emotional support whenever I needed it. Thank you for taking care of our daughter Alice and giving me the time I needed to finish this work. Jag älskar dig! Special thanks to our fabulous daughter **Alice**. She reminds me every day that the greatest thing in life is my family!

References

Agholme, L., Lindstrom, T., Kagedal, K., Marcusson, J., & Hallbeck, M. (2010). An in vitro model for neuroscience: differentiation of SH-SY5Y cells into cells with morphological and biochemical characteristics of mature neurons. *J Alzheimers Dis, 20*(4), 1069-1082.

Alves, E., Summavielle, T., Alves, C. J., Custódio, J. B., Fernandes, E., de Lourdes Bastos, M., . . . Carvalho, F. (2009). Ecstasy-induced oxidative stress to adolescent rat brain mitochondria in vivo: influence of monoamine oxidase type A. *Addict Biol, 14*(2), 185-193.

Amin-Zaki, L., Elhassani, S., Majeed, M. A., Clarkson, T. W., Doherty, R. A., & Greenwood, M. (1974). Intra-uterine methylmercury poisoning in Iraq. *Pediatrics, 54*(5), 587-595.

Anneken, J. H., & Gudelsky, G. A. (2012). MDMA produces a delayed and sustained increase in the extracellular concentration of glutamate in the rat hippocampus. *Neuropharmacology, 63*(6), 1022-1027.

Anneken, J. H., Cunningham, J. I., Collins, S. A., Yamamoto, B. K., & Gudelsky, G. A. (2013). MDMA increases glutamate release and reduces parvalbumin-positive GABAergic cells in the dorsal hippocampus of the rat: role of cyclooxygenase. *J Neuroimmune Pharmacol, 8*(1), 58-65.

Arbo, M. D., Silva, R., Barbosa, D. J., da Silva, D. D., Rossato, L. G., Bastos Mde, L., & Carmo, H. (2014). Piperazine designer drugs induce toxicity in cardiomyoblast h9c2 cells through mitochondrial impairment. *Toxicol Lett, 229*(1), 178-189.

Arbo, M. D., Silva, R., Barbosa, D. J., da Silva, D. D., Silva, S. P., Teixeira, J. P., . . . Carmo, H. (2016). In vitro neurotoxicity evaluation of piperazine designer drugs in differentiated human neuroblastoma SH-SY5Y cells. *J Appl Toxicol, 36*(1), 121-130.

Arias, C., Becerra-Garcia, F., Arrieta, I., & Tapia, R. (1998). The protein phosphatase inhibitor okadaic acid induces heat shock protein expression and neurodegeneration in rat hippocampus in vivo. *Exp Neurol, 153*(2), 242-254.

Arias, C., Sharma, N., Davies, P., & Shafit-Zagardo, B. (1993). Okadaic acid induces early changes in microtubule-associated protein 2 and tau phosphorylation prior to neurodegeneration in cultured cortical neurons. *J Neurochem, 61*(2), 673-682.

Attoff, K., Kertika, D., Lundqvist, J., Oredsson, S., & Forsby, A. (2016). Acrylamide affects proliferation and differentiation of the neural progenitor cell

line C17.2 and the neuroblastoma cell line SH-SY5Y. *Toxicol In Vitro, 35*, 100-111.

Bachmann, M., Myers, J. E., & Bezuidenhout, B. N. (1992). Acrylamide monomer and peripheral neuropathy in chemical workers. *Am J Ind Med, 21*(2), 217-222.

Barber, D. S., & LoPachin, R. M. (2004). Proteomic analysis of acrylamide-protein adduct formation in rat brain synaptosomes. *Toxicol Appl Pharmacol, 201*(2), 120-136.

Barber, D. S., Stevens, S., & LoPachin, R. M. (2007). Proteomic analysis of rat striatal synaptosomes during acrylamide intoxication at a low dose rate. *Toxicol Sci, 100*(1), 156-167.

Barbosa, D. J., Capela, J. P., Silva, R., Ferreira, L. M., Branco, P. S., Fernandes, E., . . . Carvalho, F. (2014). "Ecstasy"-induced toxicity in SH-SY5Y differentiated cells: role of hyperthermia and metabolites. *Arch Toxicol, 88*(2), 515-531.

Baskey, J. C., Kalisch, B. E., Davis, W. L., Meakin, S. O., & Rylett, R. J. (2002). PC12nnr5 cells expressing TrkA receptors undergo morphological but not cholinergic phenotypic differentiation in response to nerve growth factor. *J Neurochem, 80*(3), 501-511.

Battaglia, G., Yeh, S. Y., O'Hearn, E., Molliver, M. E., Kuhar, M. J., & De Souza, E. B. (1987). 3,4-Methylenedioxymethamphetamine and 3,4-methylenedioxyamphetamine destroy serotonin terminals in rat brain: quantification of neurodegeneration by measurement of [3H]paroxetine-labeled serotonin uptake sites. *J Pharmacol Exp Ther, 242*(3), 911-916.

Baumann, M. H., Clark, R. D., Budzynski, A. G., Partilla, J. S., Blough, B. E., & Rothman, R. B. (2005). N-substituted piperazines abused by humans mimic the molecular mechanism of 3,4-methylenedioxymethamphetamine (MDMA, or 'Ecstasy'). *Neuropsychopharmacology, 30*(3), 550-560.

Berridge, M. V., & Tan, A. S. (1993). Characterization of the cellular reduction of 3-(4,5-dimethylthiazol-2-yl)-2,5-diphenyltetrazolium bromide (MTT): subcellular localization, substrate dependence, and involvement of mitochondrial electron transport in MTT reduction. *Arch Biochem Biophys, 303*(2), 474-482.

Berridge, M. V., Herst, P. M., & Tan, A. S. (2005). Tetrazolium dyes as tools in cell biology: new insights into their cellular reduction. *Biotechnol Annu Rev, 11*, 127-152.

Bialojan, C., & Takai, A. (1988). Inhibitory effect of a marine-sponge toxin, okadaic acid, on protein phosphatases. Specificity and kinetics. *Biochem J, 256*(1), 283-290.

Biedler, J. L., Helson, L., & Spengler, B. A. (1973). Morphology and growth, tumorigenicity, and cytogenetics of human neuroblastoma cells in continuous culture. *Cancer Res, 33*(11), 2643-2652.

Biedler, J. L., Roffler-Tarlov, S., Schachner, M., & Freedman, L. S. (1978). Multiple neurotransmitter synthesis by human neuroblastoma cell lines and clones. *Cancer Res, 38*(11 Pt 1), 3751-3757.

Blaauboer, B. J. (2002). The applicability of in vitro-derived data in hazard identification and characterisation of chemicals. *Environ Toxicol Pharmacol, 11*(3-4), 213-225.

Boncler, M., Rozalski, M., Krajewska, U., Podsedek, A., & Watala, C. (2014). Comparison of PrestoBlue and MTT assays of cellular viability in the assessment of anti-proliferative effects of plant extracts on human endothelial cells. *J Pharmacol Toxicol Methods, 69*(1), 9-16.

Bye, C., Munro-Faure, A. D., Peck, A. W., & Young, P. A. (1973). A comparison of the effects of 1-benzylpiperazine and dexamphetamine on human performance tests. *Eur J Clin Pharmacol, 6*(3), 163-169.

Caballero, B., Olguin, N., Campos, F., Farina, M., Ballester, F., Lopez-Espinosa, M. J., . . . Suñol, C. (2016). Methylmercury-induced developmental toxicity is associated with oxidative stress and cofilin phosphorylation. Cellular and human studies. *Neurotoxicology*.

Cagnoli, C. M., Kharlamov, E., Atabay, C., Uz, T., & Manev, H. (1996). Apoptosis induced in neuronal cultures by either the phosphatase inhibitor okadaic acid or the kinase inhibitor staurosporine is attenuated by isoquinolinesulfonamides H-7, H-8, and H-9. *J Mol Neurosci, 7*(1), 65-76.

Capela, J. P., da Costa Araujo, S., Costa, V. M., Ruscher, K., Fernandes, E., Bastos Mde, L., . . . Carvalho, F. (2013). The neurotoxicity of hallucinogenic amphetamines in primary cultures of hippocampal neurons. *Neurotoxicology, 34*, 254-263.

Capela, J. P., Macedo, C., Branco, P. S., Ferreira, L. M., Lobo, A. M., Fernandes, E., . . . Carvalho, F. (2007). Neurotoxicity mechanisms of thioether ecstasy metabolites. *Neuroscience, 146*(4), 1743-1757.

Capela, J. P., Ruscher, K., Lautenschlager, M., Freyer, D., Dirnagl, U., Gaio, A. R., . . . Carvalho, F. (2006). Ecstasy-induced cell death in cortical neuronal cultures is serotonin 2A-receptor-dependent and potentiated under hyperthermia. *Neuroscience, 139*(3), 1069-1081.

Carratu, M. R., Borracci, P., Coluccia, A., Giustino, A., Renna, G., Tomasini, M. C., . . . Ferraro, L. (2006). Acute exposure to methylmercury at two developmental

windows: focus on neurobehavioral and neurochemical effects in rat offspring. *Neuroscience, 141*(3), 1619-1629.

Castoldi, A. F., Coccini, T., Ceccatelli, S., & Manzo, L. (2001). Neurotoxicity and molecular effects of methylmercury. *Brain Res Bull, 55*(2), 197-203.

Cattaneo, A., Biocca, S., Nasi, S., & Calissano, P. (1983). Hidden receptors for nerve growth factor in PC12 cells. *Eur J Biochem, 135*(2), 285-290.

Center for Behavioral Health Statistics and Quality. (2015). *Behavioural health trends in the United States: Results from 2014 National Survey on Drug use and Health.* Rockville, MD, USA.

Chiou, J. Y., & Westhead, E. W. (1992). Okadaic acid, a protein phosphatase inhibitor, inhibits nerve growth factor-directed neurite outgrowth in PC12 cells. *J Neurochem, 59*(5), 1963-1966.

Cho, S., & Yoon, J. Y. (2017). Organ-on-a-chip for assessing environmental toxicants. *Curr Opin Biotechnol, 45*, 34-42.

Clayden, M. G., Arsenault, L. M., Kidd, K. A., O'Driscoll, N. J., & Mallory, M. L. (2015). Mercury bioaccumulation and biomagnification in a small Arctic polynya ecosystem. *Sci Total Environ, 509-510,* 206-215.

Colado, M. I., O'Shea, E., Granados, R., Murray, T. K., & Green, A. R. (1997). In vivo evidence for free radical involvement in the degeneration of rat brain 5-HT following administration of MDMA ('ecstasy') and p-chloroamphetamine but not the degeneration following fenfluramine. *Br J Pharmacol, 121*(5), 889-900.

Das, K. P., Freudenrich, T. M., & Mundy, W. R. (2004). Assessment of PC12 cell differentiation and neurite growth: a comparison of morphological and neurochemical measures. *Neurotoxicol Teratol, 26*(3), 397-406.

Das, V., & Miller, J. H. (2012). Microtubule stabilization by peloruside A and paclitaxel rescues degenerating neurons from okadaic acid-induced tau phosphorylation. *Eur J Neurosci, 35*(11), 1705-1717.

de Boer, D., Bosman, I. J., Hidvegi, E., Manzoni, C., Benko, A. A., dos Reys, L. J., & Maes, R. A. (2001). Piperazine-like compounds: a new group of designer drugs-of-abuse on the European market. *Forensic Sci Int, 121(1-2)*, 47-56.

Dengler, W. A., Schulte, J., Berger, D. P., Mertelsmann, R., & Fiebig, H. H. (1995). Development of a propidium iodide fluorescence assay for proliferation and cytotoxicity assays. *Anticancer Drugs, 6*(4), 522-532.

Dias da Silva, D., Silva, M. J., Moreira, P., Martins, M. J., Valente, M. J., Carvalho, F., . . . Carmo, H. (2017). In vitro hepatotoxicity of 'Legal X': the combination of 1-benzylpiperazine (BZP) and 1-(m-trifluoromethylphenyl)piperazine (TFMPP)

triggers oxidative stress, mitochondrial impairment and apoptosis. *Arch Toxicol, 91*(3): 1413-1430

Dias da Silva, D., Arbo, M. D., Valente, M. J., Bastos, M. L., & Carmo, H. (2015). Hepatotoxicity of piperazine designer drugs: Comparison of different in vitro models. *Toxicol In Vitro, 29*(5), 987-996.

Ekino, S., Susa, M., Ninomiya, T., Imamura, K., & Kitamura, T. (2007). Minamata disease revisited: an update on the acute and chronic manifestations of methyl mercury poisoning. *J Neurol Sci, 262*(1-2), 131-144.

EMCDDA. (2009). *Report on the risk assessment of BZP in the framework of the Council decision on new psychoactive substances.* Luxembourg: Office for Official Publications of the European Communities.

Fantegrossi, W. E., Godlewski, T., Karabenick, R. L., Stephens, J. M., Ullrich, T., Rice, K. C., & Woods, J. H. (2003). Pharmacological characterization of the effects of 3,4-methylenedioxymethamphetamine ("ecstasy") and its enantiomers on lethality, core temperature, and locomotor activity in singly housed and crowded mice. *Psychopharmacology (Berl)*, *166*(3), 202-211.

Fantegrossi, W. E., Winger, G., Woods, J. H., Woolverton, W. L., & Coop, A. (2005). Reinforcing and discriminative stimulus effects of 1-benzylpiperazine and trifluoromethylphenylpiperazine in rhesus monkeys. *Drug Alcohol Depend, 77*(2), 161-168.

FDA (U.S. Food and Drug Administration) (2017). Mercury concentration in fish: FDA monitoring program (1990-2010). Retrieved from http://www.fda.gov /Food/ FoodborneIllness Contaminants/Metals/ucm191007.htm.

Finley, M. F., Kulkarni, N., & Huettner, J. E. (1996). Synapse formation and establishment of neuronal polarity by P19 embryonic carcinoma cells and embryonic stem cells. *J Neurosci, 16*(3), 1056-1065.

Fitzgerald, J. L., & Reid, J. J. (1990). Effects of methylenedioxymethamphetamine on the release of monoamines from rat brain slices. *Eur J Pharmacol*, *191*(2), 217-220.

Forman, R. F., Marlowe, D. B., & McLellan, A. T. (2006). The Internet as a source of drugs of abuse. *Curr Psychiatry Rep, 8*(5), 377-382.

Fowler, C. J., O'Neill, C., Almqvist, P., Nilsson, S., Wiehager, B., & Winblad, B. (1989). Muscarinic receptors coupled to inositol phospholipid breakdown in human SH-SY5Y neuroblastoma cells: Effect of retinoic acid-induced differentiation. *Neurochem Int, 15*(1), 73-79.

Fujimura, M., & Usuki, F. (2015). Low concentrations of methylmercury inhibit neural progenitor cell proliferation associated with up-regulation of glycogen synthase kinase 3β and subsequent degradation of cyclin E in rats. *Toxicol Appl Pharmacol, 288*(1), 19-25.

Fujimura, M., Usuki, F., Cheng, J., & Zhao, W. (2016). Prenatal low-dose methylmercury exposure impairs neurite outgrowth and synaptic protein expression and suppresses TrkA pathway activity and eEF1A1 expression in the rat cerebellum. *Toxicol Appl Pharmacol, 298*, 1-8.

Fujita, K., Lazarovici, P., & Guroff, G. (1989). Regulation of the differentiation of PC12 pheochromocytoma cells. *Environ Health Perspect, 80*, 127-142.

Gee, P., Gilbert, M., Richardson, S., Moore, G., Paterson, S., & Graham, P. (2008). Toxicity from the recreational use of 1-benzylpiperazine. *Clin Toxicol (Phila), 46*(9), 802-807.

Gee, P., Jerram, T., & Bowie, D. (2010). Multiorgan failure from 1-benzylpiperazine ingestion--legal high or lethal high? *Clin Toxicol (Phila), 48*(3), 230-233.

Gee, P., Richardson, S., Woltersdorf, W., & Moore, G. (2005). Toxic effects of BZP-based herbal party pills in humans: a prospective study in Christchurch, New Zealand. *N Z Med J, 118*(1227), U1784.

Granado, N., O'Shea, E., Bove, J., Vila, M., Colado, M. I., & Moratalla, R. (2008). Persistent MDMA-induced dopaminergic neurotoxicity in the striatum and substantia nigra of mice. *J Neurochem, 107*(4), 1102-1112.

Grandjean, P., Weihe, P., White, R. F., Debes, F., Araki, S., Yokoyama, K., . . . Jorgensen, P. J. (1997). Cognitive deficit in 7-year-old children with prenatal exposure to methylmercury. *Neurotoxicol Teratol, 19*(6), 417-428.

Green, A. R., O'Shea, E., Saadat, K. S., Elliott, J. M., & Colado, M. I. (2005). Studies on the effect of MDMA ('ecstasy') on the body temperature of rats housed at different ambient room temperatures. *Br J Pharmacol*, *146*(2), 306-312.

Greene, L. A., & Rein, G. (1977). Synthesis, storage and release of acetylcholine by a noradrenergic pheochromocytoma cell line. *Nature, 268*(5618), 349-351.

Greene, L. A., & Tischler, A. S. (1976). Establishment of a noradrenergic clonal line of rat adrenal pheochromocytoma cells which respond to nerve growth factor. *Proc Natl Acad Sci U S A, 73*(7), 2424-2428.

Gudelsky, G. A., & Nash, J. F. (1996). Carrier-mediated release of serotonin by 3,4-methylenedioxymethamphetamine: implications for serotonin-dopamine interactions. *J Neurochem, 66*(1), 243-249.

Guo, B. Q., Yan, C. H., Cai, S. Z., Yuan, X. B., & Shen, X. M. (2013). Low level prenatal exposure to methylmercury disrupts neuronal migration in the developing rat cerebral cortex. *Toxicology, 304,* 57-68.

Gustafsson, H., Runesson, J., Lundqvist, J., Lindegren, H., Axelsson, V., & Forsby, A. (2010). Neurofunctional endpoints assessed in human neuroblastoma SH-SY5Y cells for estimation of acute systemic toxicity. *Toxicol Appl Pharmacol, 245*(2), 191-202.

Hagino, Y., Takamatsu, Y., Yamamoto, H., Iwamura, T., Murphy, D. L., Uhl, G. R., . . . Ikeda, K. (2011). Effects of MDMA on Extracellular Dopamine and Serotonin Levels in Mice Lacking Dopamine and/or Serotonin Transporters. *Curr Neuropharmacol, 9*(1), 91-95.

Hall, A. P., & Henry, J. A. (2006). Acute toxic effects of 'Ecstasy' (MDMA) and related compounds: overview of pathophysiology and clinical management. *Br J Anaesth*, *96*(6), 678-685.

Hamblin, M. W., Adriaenssens, P. I., Ariani, K., Cawthon, R. M., Stratford, C. A., Tan, G. L., & Ciaranello, R. D. (1987). Ascorbic acid prevents nonreceptor "specific" binding of [3H]-5-hydroxytryptamine to bovine cerebral cortex membranes. *J Pharmacol Exp Ther, 240*(3), 701-711.

Harada, M. (1995). Minamata disease: methylmercury poisoning in Japan caused by environmental pollution. *Crit Rev Toxicol, 25*(1), 1-24.

Harry, G. J., & Tiffany-Castiglioni, E. (2005). Evaluation of neurotoxic potential by use of in vitro systems. *Expert Opin Drug Metab Toxicol, 1*(4), 701-713.

Hartung, T. K., Schofield, E., Short, A. I., Parr, M. J., & Henry, J. A. (2002). Hyponatraemic states following 3,4-methylenedioxymethamphetamine (MDMA, 'ecstasy') ingestion. *QJM, 95*(7), 431-437.

Haystead, T. A., Sim, A. T., Carling, D., Honnor, R. C., Tsukitani, Y., Cohen, P., & Hardie, D. G. (1989). Effects of the tumour promoter okadaic acid on intracellular protein phosphorylation and metabolism. *Nature, 337*(6202), 78-81.

He, F. S., Zhang, S. L., Wang, H. L., Li, G., Zhang, Z. M., Li, F. L., . . . Hu, F. R. (1989). Neurological and electroneuromyographic assessment of the adverse effects of acrylamide on occupationally exposed workers. *Scand J Work Environ Health, 15*(2), 125-129.

Henry, J. A., Jeffreys, K. J., & Dawling, S. (1992). Toxicity and deaths from 3,4-methylenedioxymethamphetamine ("ecstasy"). *Lancet, 340*(8816), 384-387.

Hu, B. Y., Weick, J. P., Yu, J., Ma, L. X., Zhang, X. Q., Thomson, J. A., & Zhang, S. C. (2010). Neural differentiation of human induced pluripotent stem cells follows developmental principles but with variable potency. *Proc Natl Acad Sci U S A, 107*(9), 4335-4340.

Invitrogen. (2012). PrestoBlue® cell viability reagent frequently asked questions. Retrieved from https://tools.thermofisher.com/content/sfs/manuals/PrestoBlue FAQ.pdf.

Jaako-Movits, K., Zharkovsky, T., Romantchik, O., Jurgenson, M., Merisalu, E., Heidmets, L. T., & Zharkovsky, A. (2005). Developmental lead exposure impairs contextual fear conditioning and reduces adult hippocampal neurogenesis in the rat brain. *Int J Dev Neurosci, 23*(7), 627-635.

Jangir, B. L., Mahaprabhu, R., Rahangadale, S., Bhandarkar, A. G., & Kurkure, N. V. (2016). Neurobehavioral alterations and histopathological changes in brain and spinal cord of rats intoxicated with acrylamide. *Toxicol Ind Health, 32*(3), 526-540.

Johnson, M. P., Conarty, P. F., & Nichols, D. E. (1991). [3H]monoamine releasing and uptake inhibition properties of 3,4-methylenedioxymethamphetamine and p-chloroamphetamine analogues. *Eur J Pharmacol*, *200*(1), 9-16.

Jones-Villeneuve, E. M., McBurney, M. W., Rogers, K. A., & Kalnins, V. I. (1982). Retinoic acid induces embryonal carcinoma cells to differentiate into neurons and glial cells. *J Cell Biol, 94*(2), 253-262.

Judson, R., Houck, K., Martin, M., Knudsen, T., Thomas, R. S., Sipes, N., . . . Crofton, K. (2014). In vitro and modelling approaches to risk assessment from the U.S. Environmental Protection Agency ToxCast programme. *Basic Clin Pharmacol Toxicol, 115*(1), 69-76.

Julshamn, K., Andersen, A., Ringdal, O., & Morkore, J. (1987). Trace elements intake in the Faroe Islands. I. Element levels in edible parts of pilot whales (Globicephalus meleanus). *Sci Total Environ, 65*, 53-62.

Kamat, P. K., Rai, S., Swarnkar, S., Shukla, R., & Nath, C. (2014). Molecular and cellular mechanism of okadaic acid (OKA)-induced neurotoxicity: a novel tool for Alzheimer's disease therapeutic application. *Mol Neurobiol, 50*(3), 852-865.

Kamat, P. K., Tota, S., Shukla, R., Ali, S., Najmi, A. K., & Nath, C. (2011). Mitochondrial dysfunction: a crucial event in okadaic acid (ICV) induced

memory impairment and apoptotic cell death in rat brain. *Pharmacol Biochem Behav, 100*(2), 311-319.

Katsetos, C. D., Legido, A., Perentes, E., & Mork, S. J. (2003). Class III beta-tubulin isotype: a key cytoskeletal protein at the crossroads of developmental neurobiology and tumor neuropathology. *J Child Neurol, 18*(12), 851-866; discussion 867.

Katz, D. M., & Kimelberg, H. K. (1985). Kinetics and autoradiography of high affinity uptake of serotonin by primary astrocyte cultures. *J Neurosci, 5*(7), 1901-1908.

Ko, M. H., Chen, W. P., Lin-Shiau, S. Y., & Hsieh, S. T. (1999). Age-dependent acrylamide neurotoxicity in mice: morphology, physiology, and function. *Exp Neurol, 158*(1), 37-46.

Komoike, Y., & Matsuoka, M. (2016). Endoplasmic reticulum stress-mediated neuronal apoptosis by acrylamide exposure. *Toxicol Appl Pharmacol, 310*, 68-77.

Korecka, J. A., van Kesteren, R. E., Blaas, E., Spitzer, S. O., Kamstra, J. H., Smit, A. B., . . . Bossers, K. (2013). Phenotypic characterization of retinoic acid differentiated SH-SY5Y cells by transcriptional profiling. *PLoS One, 8*(5), e63862.

Lakshmi, D., Gopinath, K., Jayanthy, G., Anjum, S., Prakash, D., & Sudhandiran, G. (2012). Ameliorating effect of fish oil on acrylamide induced oxidative stress and neuronal apoptosis in cerebral cortex. *Neurochem Res, 37*(9), 1859-1867.

Lall, N., Henley-Smith, C. J., De Canha, M. N., Oosthuizen, C. B., & Berrington, D. (2013). Viability Reagent, PrestoBlue, in Comparison with Other Available Reagents, Utilized in Cytotoxicity and Antimicrobial Assays. *Int J Microbiol, 2013*, 420601.

Leonardi, E. T., & Azmitia, E. C. (1994). MDMA (ecstasy) inhibition of MAO type A and type B: comparisons with fenfluramine and fluoxetine (Prozac). *Neuropsychopharmacology, 10*(4), 231-238.

Lichtenfels, R., Biddison, W. E., Schulz, H., Vogt, A. B., & Martin, R. (1994). CARE-LASS (calcein-release-assay), an improved fluorescence-based test system to measure cytotoxic T lymphocyte activity. *J Immunol Methods, 172*(2), 227-239.

Limke, T. L., & Atchison, W. D. (2002). Acute exposure to methylmercury opens the mitochondrial permeability transition pore in rat cerebellar granule cells. *Toxicol Appl Pharmacol, 178*(1), 52-61.

Logan, B. J., Laverty, R., Sanderson, W. D., & Yee, Y. B. (1988). Differences between rats and mice in MDMA (methylenedioxymethylamphetamine) neurotoxicity. *Eur J Pharmacol, 152*(3), 227-234.

LoPachin, R. M., & Barber, D. S. (2006). Synaptic cysteine sulfhydryl groups as targets of electrophilic neurotoxicants. *Toxicol Sci, 94*(2), 240-255.

LoPachin, R. M., & Gavin, T. (2012). Molecular mechanism of acrylamide neurotoxicity: lessons learned from organic chemistry. *Environ Health Perspect, 120*(12), 1650-1657.

LoPachin, R. M., Schwarcz, A. I., Gaughan, C. L., Mansukhani, S., & Das, S. (2004). In vivo and in vitro effects of acrylamide on synaptosomal neurotransmitter uptake and release. *Neurotoxicology, 25*(3), 349-363.

Lopes, F. M., Schroder, R., da Frota, M. L., Jr., Zanotto-Filho, A., Muller, C. B., Pires, A. S., . . . Klamt, F. (2010). Comparison between proliferative and neuron-like SH-SY5Y cells as an in vitro model for Parkinson disease studies. *Brain Res, 1337*, 85-94.

Lu, L., Zhang, L., Wai, M. S., Yew, D. T., & Xu, J. (2012). Exocytosis of MTT formazan could exacerbate cell injury. *Toxicol In Vitro, 26*(4), 636-644.

Malberg, J. E., & Seiden, L. S. (1998). Small changes in ambient temperature cause large changes in 3,4-methylenedioxymethamphetamine (MDMA)-induced serotonin neurotoxicity and core body temperature in the rat. *J Neurosci, 18*(13), 5086-5094.

Manfroi, C. B., Schwalm, F. D., Cereser, V., Abreu, F., Oliveira, A., Bizarro, L., . . . Farina, M. (2004). Maternal milk as methylmercury source for suckling mice: neurotoxic effects involved with the cerebellar glutamatergic system. *Toxicol Sci, 81*(1), 172-178.

McBurney, M. W., & Rogers, B. J. (1982). Isolation of male embryonal carcinoma cells and their chromosome replication patterns. *Dev Biol, 89*(2), 503-508.

McBurney, M. W., Jones-Villeneuve, E. M., Edwards, M. K., & Anderson, P. J. (1982). Control of muscle and neuronal differentiation in a cultured embryonal carcinoma cell line. *Nature, 299*(5879), 165-167.

McBurney, M. W., Reuhl, K. R., Ally, A. I., Nasipuri, S., Bell, J. C., & Craig, J. (1988). Differentiation and maturation of embryonal carcinoma-derived neurons in cell culture. *Journal of Neuroscience, 8*(3), 1063-1073.

McMillan, C. R., Sharma, R., Ottenhof, T., & Niles, L. P. (2007). Modulation of tyrosine hydroxylase expression by melatonin in human SH-SY5Y neuroblastoma cells. *Neurosci Lett, 419*(3), 202-206.

Meamar, R., Karamali, F., Mousavi, S. A., Baharvand, H., & Nasr-Esfahani, M. H. (2012). Could MDMA Promote Stemness Characteristics in Mouse Embryonic Stem Cells via mGlu5 Metabotropic Glutamate Receptors? *Cell J, 14*(3), 185-192.

Meamar, R., Karamali, F., Sadeghi, H. M., Etebari, M., Nasr-Esfahani, M. H., & Baharvand, H. (2010). Toxicity of ecstasy (MDMA) towards embryonic stem cell-derived cardiac and neural cells. *Toxicol In Vitro, 24*(4), 1133-1138.

Meijering, E., Jacob, M., Sarria, J. C., Steiner, P., Hirling, H., & Unser, M. (2004). Design and validation of a tool for neurite tracing and analysis in fluorescence microscopy images. *Cytometry A, 58*(2), 167-176.

Merrick, S. E., Trojanowski, J. Q., & Lee, V. M. (1997). Selective destruction of stable microtubules and axons by inhibitors of protein serine/threonine phosphatases in cultured human neurons. *J Neurosci, 17*(15), 5726-5737.

Milroy, C. M., Clark, J. C., & Forrest, A. R. (1996). Pathology of deaths associated with "ecstasy" and "eve" misuse. *J Clin Pathol, 49*(2), 149-153.

Morassutti, D. J., Staines, W. A., Magnuson, D. S., Marshall, K. C., & McBurney, M. W. (1994). Murine embryonal carcinoma-derived neurons survive and mature following transplantation into adult rat striatum. *Neuroscience, 58*(4), 753-763.

Mosmann, T. (1983). Rapid colorimetric assay for cellular growth and survival: application to proliferation and cytotoxicity assays. *J Immunol Methods, 65*(1-2), 55-63.

Mounteney, J., Griffiths, P., Sedefov, R., Noor, A., Vicente, J., & Simon, R. (2016). The drug situation in Europe: an overview of data available on illicit drugs and new psychoactive substances from European monitoring in 2015. *Addiction, 111*(1), 34-48.

Nagai, F., Nonaka, R., & Satoh Hisashi Kamimura, K. (2007). The effects of non-medically used psychoactive drugs on monoamine neurotransmission in rat brain. *Eur J Pharmacol, 559*(2-3), 132-137.

Nagatsu, T. (2004). Progress in monoamine oxidase (MAO) research in relation to genetic engineering. *Neurotoxicology, 25*(1-2), 11-20.

Neri, S., Mariani, E., Meneghetti, A., Cattini, L., & Facchini, A. (2001). Calcein-acetyoxymethyl cytotoxicity assay: standardization of a method allowing

additional analyses on recovered effector cells and supernatants. *Clin Diagn Lab Immunol, 8*(6), 1131-1135.

Nielsen, L. T., Hansen, P. J., Krock, B., & Vismann, B. (2016). Accumulation, transformation and breakdown of DSP toxins from the toxic dinoflagellate Dinophysis acuta in blue mussels, Mytilus edulis. *Toxicon, 117*, 84-93.

O'Callaghan, J. P., & Miller, D. B. (1994). Neurotoxicity profiles of substituted amphetamines in the C57BL/6J mouse. *J Pharmacol Exp Ther, 270*(2), 741-751.

O'Hearn, E., Battaglia, G., De Souza, E. B., Kuhar, M. J., & Molliver, M. E. (1988). Methylenedioxyamphetamine (MDA) and methylenedioxymethamphetamine (MDMA) cause selective ablation of serotonergic axon terminals in forebrain: immunocytochemical evidence for neurotoxicity. *J Neurosci, 8*(8), 2788-2803.

Olson, H., Betton, G., Robinson, D., Thomas, K., Monro, A., Kolaja, G., . . . Heller, A. (2000). Concordance of the toxicity of pharmaceuticals in humans and in animals. *Regul Toxicol Pharmacol, 32*(1), 56-67.

Orio, L., O'Shea, E., Sanchez, V., Pradillo, J. M., Escobedo, I., Camarero, J., . . . Colado, M. I. (2004). 3,4-Methylenedioxymethamphetamine increases interleukin-1beta levels and activates microglia in rat brain: studies on the relationship with acute hyperthermia and 5-HT depletion. *J Neurochem, 89*(6), 1445-1453.

Pallanti, S., & Mazzi, D. (1992). MDMA (Ecstasy) precipitation of panic disorder. *Biol Psychiatry, 32*(1), 91-95.

Pan, X., Zhu, L., Lu, H., Wang, D., Lu, Q., & Yan, H. (2015). Melatonin Attenuates Oxidative Damage Induced by Acrylamide In Vitro and In Vivo. *Oxid Med Cell Longev*, 2015, 703709.

Parks, J. M., Johs, A., Podar, M., Bridou, R., Hurt, R. A., Jr., Smith, S. D., . . . Liang, L. (2013). The genetic basis for bacterial mercury methylation. *Science, 339*(6125), 1332-1335.

Parnas, D., & Linial, M. (1995). Cholinergic properties of neurons differentiated from an embryonal carcinoma cell-line (P19). *Int J Dev Neurosci, 13*(7), 767-781.

Parran, D. K., Barone, S., Jr., & Mundy, W. R. (2003). Methylmercury decreases NGF-induced TrkA autophosphorylation and neurite outgrowth in PC12 cells. *Brain Res Dev Brain Res, 141*(1-2), 71-81.

Parrott, A. C. (2002). Recreational Ecstasy/MDMA, the serotonin syndrome, and serotonergic neurotoxicity. *Pharmacol Biochem Behav, 71*(4), 837-844.

Pentney, A. R. (2001). An exploration of the history and controversies surrounding MDMA and MDA. *J Psychoactive Drugs*, *33*(3), 213-221.

Peroutka, S. J., Newman, H., & Harris, H. (1988). Subjective effects of 3,4-methylenedioxymethamphetamine in recreational users. *Neuropsychopharmacology, 1*(4), 273-277.

Perry, S. W., Norman, J. P., Barbieri, J., Brown, E. B., & Gelbard, H. A. (2011). Mitochondrial membrane potential probes and the proton gradient: a practical usage guide. *Biotechniques, 50*(2), 98-115.

Puerta, E., Hervias, I., Goñi-Allo, B., Zhang, S. F., Jordán, J., Starkov, A. A., & Aguirre, N. (2010). Methylenedioxymethamphetamine inhibits mitochondrial complex I activity in mice: a possible mechanism underlying neurotoxicity. *Br J Pharmacol, 160*(2), 233-245.

Radio, N. M., & Mundy, W. R. (2008). Developmental neurotoxicity testing in vitro: models for assessing chemical effects on neurite outgrowth. *Neurotoxicology, 29*(3), 361-376.

Ricaurte, G. A., Forno, L. S., Wilson, M. A., DeLanney, L. E., Irwin, I., Molliver, M. E., & Langston, J. W. (1988). (+/-)3,4-Methylenedioxymethamphetamine selectively damages central serotonergic neurons in nonhuman primates. *JAMA, 260*(1), 51-55.

Rieger, F., Shelanski, M. L., & Greene, L. A. (1980). The effects of nerve growth factor on acetylcholinesterase and its multiple forms in cultures of rat PC12 pheochromocytoma cells: increased total specific activity and appearance of the 16 S molecular form. *Dev Biol, 76*(1), 238-243.

Roden, M. M., Lee, K. H., Panelli, M. C., & Marincola, F. M. (1999). A novel cytolysis assay using fluorescent labeling and quantitative fluorescent scanning technology. *J Immunol Methods, 226*(1-2), 29-41.

Rudd, M. L., Nicolas, A. N., Brown, B. L., Fischer-Stenger, K., & Stewart, J. K. (2005). Peritoneal macrophages express the serotonin transporter. *J Neuroimmunol, 159*(1-2), 113-118.

Sanfeliu, C., Sebastia, J., & Ki, S. U. (2001). Methylmercury neurotoxicity in cultures of human neurons, astrocytes, neuroblastoma cells. *Neurotoxicology, 22*(3), 317-327.

Sasaki, K., Murata, M., Yasumoto, T., Mieskes, G., & Takai, A. (1994). Affinity of okadaic acid to type-1 and type-2A protein phosphatases is markedly reduced by oxidation of its 27-hydroxyl group. *Biochem J, 298*(Pt2), 259-262.

Schaefer, J. K., Rocks, S. S., Zheng, W., Liang, L., Gu, B., & Morel, F. M. (2011). Active transport, substrate specificity, and methylation of Hg(II) in anaerobic bacteria. *Proc Natl Acad Sci U S A, 108*(21), 8714-8719.

Schubert, D., Heinemann, S., & Kidokoro, Y. (1977). Cholinergic metabolism and synapse formation by a rat nerve cell line. *Proc Natl Acad Sci U S A, 74*(6), 2579-2583.

Schwartz, M. P., Hou, Z., Propson, N. E., Zhang, J., Engstrom, C. J., Santos Costa, V., . . . Thomson, J. A. (2015). Human pluripotent stem cell-derived neural constructs for predicting neural toxicity. *Proc Natl Acad Sci U S A, 112*(40), 12516-12521.

Shankaran, M., Yamamoto, B. K., & Gudelsky, G. A. (1999). Involvement of the serotonin transporter in the formation of hydroxyl radicals induced by 3,4-methylenedioxymethamphetamine. *Eur J Pharmacol, 385*(2-3), 103-110.

Sharma, S., & Notter, M. F. (1988). Characterization of neurotransmitter phenotype during neuronal differentiation of embryonal carcinoma cells. *Dev Biol, 125*(2), 246-254.

Sharp, D. (2003). Acrylamide in food. *Lancet, 361*(9355), 361-362.

Sheehan, M. C., Burke, T. A., Navas-Acien, A., Breysse, P. N., McGready, J., & Fox, M. A. (2014). Global methylmercury exposure from seafood consumption and risk of developmental neurotoxicity: a systematic review. *Bull World Health Organ, 92*(4), 254-269F.

Sheridan, J., & Butler, R. (2010). "They're legal so they're safe, right?" What did the legal status of BZP-party pills mean to young people in New Zealand? *Int J Drug Policy, 21(1),* 77-81.

Shioda, K., Nisijima, K., Yoshino, T., Kuboshima, K., Iwamura, T., Yui, K., & Kato, S. (2008). Risperidone attenuates and reverses hyperthermia induced by 3,4-methylenedioxymethamphetamine (MDMA) in rats. *Neurotoxicology, 29*(6),

Slotkin, T. A., MacKillop, E. A., Ryde, I. T., Tate, C. A., & Seidler, F. J. (2007). Screening for developmental neurotoxicity using PC12 cells: comparisons of organophosphates with a carbamate, an organochlorine, and divalent nickel. *Environ Health Perspect, 115*(1), 93-101.

Smith, S. C., Reuhl, K. R., Craig, J., & McBurney, M. W. (1987). The role of aggregation in embryonal carcinoma cell differentiation. *J Cell Physiol, 131*(1), 74-84.

Sokolowski, K., Falluel-Morel, A., Zhou, X., & DiCicco-Bloom, E. (2011). Methylmercury (MeHg) elicits mitochondrial-dependent apoptosis in developing hippocampus and acts at low exposures. *Neurotoxicology, 32*(5), 535-544.

Solomon, F. (1980). Neuroblastoma cells recapitulate their detailed neurite morphologies after reversible microtubule disassembly. *Cell, 21*(2), 333-338.

Souza-Araujo, J., Giarrizzo, T., Lima, M. O., & Souza, M. B. (2016). Mercury and methyl mercury in fishes from Bacajá River (Brazilian Amazon): evidence for bioaccumulation and biomagnification. *J Fish Biol, 89*(1), 249-263.

Staines, W. A., Morassutti, D. J., Reuhl, K. R., Ally, A. I., & McBurney, M. W. (1994). Neurons derived from P19 embryonal carcinoma cells have varied morphologies and neurotransmitters. *Neuroscience, 58*(4), 735-751.

Steele, T. D., Nichols, D. E., & Yim, G. K. (1987). Stereochemical effects of 3,4-methylenedioxymethamphetamine (MDMA) and related amphetamine derivatives on inhibition of uptake of [3H]monoamines into synaptosomes from different regions of rat brain. *Biochem Pharmacol*, *36*(14), 2297-2303.

Strain, J. J., Yeates, A. J., van Wijngaarden, E., Thurston, S. W., Mulhern, M. S., McSorley, E. M., . . . Davidson, P. W. (2015). Prenatal exposure to methyl mercury from fish consumption and polyunsaturated fatty acids: associations with child development at 20 mo of age in an observational study in the Republic of Seychelles. *Am J Clin Nutr, 101*(3), 530-537.

Stringari, J., Nunes, A. K., Franco, J. L., Bohrer, D., Garcia, S. C., Dafre, A. L., . . . Farina, M. (2008). Prenatal methylmercury exposure hampers glutathione antioxidant system ontogenesis and causes long-lasting oxidative stress in the mouse brain. *Toxicol Appl Pharmacol, 227*(1), 147-154.

Substance Abuse and Mental Health Services Administration. (2013). *Drug Abuse Warning Network, 2011: National Estimates of Drug-Related Emergency Department Visits.* Rockville, MD, USA: Substance Abuse and Mental Health Services Administration.

Svensson, A. C., Johansson, M., Persson, E., Carchenilla, M. S., & Jacobsson, S. O. (2006). Expression of functional CB1 cannabinoid receptors in retinoic acid-differentiated P19 embryonal carcinoma cells. *J Neurosci Res, 83*(6), 1128-1140.

Taeymans, D., Wood, J., Ashby, P., Blank, I., Studer, A., Stadler, R. H., . . . Whitmore, T. (2004). A review of acrylamide: an industry perspective on research, analysis, formation, and control. *Crit Rev Food Sci Nutr, 44*(5), 323-347.

Takahashi, T., Deng, Y., Maruyama, W., Dostert, P., Kawai, M., & Naoi, M. (1994). Uptake of a neurotoxin-candidate, (R)-1,2-dimethyl-6,7-dihydroxy-1,2,3,4-

tetrahydroisoquinoline into human dopaminergic neuroblastoma SH-SY5Y cells by dopamine transport system. *J Neural Transm Gen Sect, 98*(2), 107-118.

Tamm, C., Duckworth, J., Hermanson, O., & Ceccatelli, S. (2006). High susceptibility of neural stem cells to methylmercury toxicity: effects on cell survival and neuronal differentiation. *J Neurochem, 97*(1), 69-78.

Thompson, I., Williams, G., Aldington, S., Williams, M., Caldwell, B., Dickson, S., . . . Beasley, R. (2006). *The benzylpiperazine (BZP)/trifluoromethylphenyl-piperazine (TFMPP) and alcohol safety study*. Wellington, New Zealand: Medical Research Institute of New Zealand.

Tian, S. M., Ma, Y. X., Shi, J., Lou, T. Y., Liu, S. S., & Li, G. Y. (2015). Acrylamide neurotoxicity on the cerebrum of weaning rats. *Neural Regen Res, 10*(6), 938-943.

Tofighi, R., Johansson, C., Goldoni, M., Ibrahim, W. N., Gogvadze, V., Mutti, A., & Ceccatelli, S. (2011). Hippocampal neurons exposed to the environmental contaminants methylmercury and polychlorinated biphenyls undergo cell death via parallel activation of calpains and lysosomal proteases. *Neurotox Res, 19*(1), 183-194.

Turetsky, D. M., Huettner, J. E., Gottlieb, D. I., Goldberg, M. P., & Choi, D. W. (1993). Glutamate receptor-mediated currents and toxicity in embryonal carcinoma cells. *J Neurobiol, 24*(9), 1157-1169.

van Wijngaarden, E., Thurston, S. W., Myers, G. J., Strain, J. J., Weiss, B., Zarcone, T., . . . Davidson, P. W. (2013). Prenatal methyl mercury exposure in relation to neurodevelopment and behavior at 19 years of age in the Seychelles Child Development Study. *Neurotoxicol Teratol, 39,* 19-25.

Weber, S., Fernández-Cachón, M. L., Nascimento, J. M., Knauer, S., Offermann, B., Murphy, R. F., . . . Busch, H. (2013). Label-free detection of neuronal differentiation in cell populations using high-throughput live-cell imaging of PC12 cells. *PLoS One, 8*(2), e56690.

Wilkins, C., Girling, M., Sweetsur, P., Huckle, T., & Huakau, J. (2006). Legal party pill use in New Zealand: Prevalence of use, availability, health harms and "gateway effects" of benzylpiperazine (BZP) and trifluoromethylphenyl-piperazine (TFMPP). Auckland: Centre for Social and Health Outcomes Research and Evaluation (SHORE), Massey University.

Wilson, M. S., Graham, J. R., & Ball, A. J. (2014). Multiparametric High Content Analysis for assessment of neurotoxicity in differentiated neuronal cell lines and human embryonic stem cell-derived neurons. *Neurotoxicology, 42*, 33-48.

Wise, L. D., Gordon, L. R., Soper, K. A., Duchai, D. M., & Morrissey, R. E. (1995). Developmental neurotoxicity evaluation of acrylamide in Sprague-Dawley rats. *Neurotoxicol Teratol, 17*(2), 189-198.

World Health Organization. (2016). Mercury and health (Fact sheet No. 361). Retrieved from: http://www.who.int/mediacentre/factsheets/fs361/en/

Xu, M., McCanna, D. J., & Sivak, J. G. (2015). Use of the viability reagent PrestoBlue in comparison with alamarBlue and MTT to assess the viability of human corneal epithelial cells. *J Pharmacol Toxicol Methods, 71*, 1-7.

Yao, M., Bain, G., & Gottlieb, D. I. (1995). Neuronal differentiation of P19 embryonal carcinoma cells in defined media. *J Neurosci Res, 41*(6), 792-804.

Yi, K. D., Covey, D. F., & Simpkins, J. W. (2009). Mechanism of okadaic acid-induced neuronal death and the effect of estrogens. *J Neurochem, 108*(3), 732-740.

Yoon, S., Choi, J., Yoon, J., Huh, J. W., & Kim, D. (2006). Okadaic acid induces JNK activation, bim overexpression and mitochondrial dysfunction in cultured rat cortical neurons. *Neurosci Lett, 394*(3), 190-195.

Zawilska, J. B. (2015). "Legal Highs"- An Emerging Epidemic of Novel Psychoactive Substances. *Int Rev Neurobiol, 120*, 273-300.

Zhang, L., Shirayama, Y., Shimizu, E., Iyo, M., & Hashimoto, K. (2006). Protective effects of minocycline on 3,4-methylenedioxymethamphetamine-induced neurotoxicity in serotonergic and dopaminergic neurons of mouse brain. *Eur J Pharmacol, 544*(1-3), 1-9.

Zhang, Z., & Simpkins, J. W. (2010). An okadaic acid-induced model of tauopathy and cognitive deficiency. *Brain Res, 1359*, 233-246.

Zuba, D., & Byrska, B. (2013). Prevalence and co-existence of active components of 'legal highs'. *Drug Test Anal, 5*(6), 420-429.